博士論文

Studies on Molecular Mechanisms of Light-Induced Stomatal Opening via Phosphorylation of the C-Terminal Auto-Inhibitory Domain of Plasma Membrane H^+-ATPase

(細胞膜 H^+-ATPase の C 末端自己阻害ドメインのリン酸化を介した光に応答した気孔開口の分子機構の研究)

2025 年 3 月
冨士彩紗
山口大学 創成科学研究科

Contents

General introduction

Adenosine triphosphate (ATP), a substance that mediates the life activities of organisms on the earth, enables cellular activities through the energy released when ATP is hydrolyzed to adenosine diphosphate (ADP) and inorganic phosphate (Pi) within cells. The source of ATP is the light energy that falls on the earth, and the only process that converts light energy into a form usable by organisms is photosynthesis, which occurs exclusively in the chloroplasts of plant cells. All living organisms on the earth rely on this plant photosynthesis for survival.

Chloroplasts are plant specific organelles differentiated from plastids and contain light-harvesting complexes for capturing light, photosystem complexes, components of the electron transport chain, and ATP synthases in the chloroplast envelope. The light reaction requires H_2O to obtain electrons from water-splitting, and this process generates a H^+ concentration gradient, resulting in ATP synthesis through ATP synthase[1,2]. This ATP is converted into sugars through the Calvin-Benson cycle, which uses CO_2 as a substrate, and is stored as starch, providing a sufficient reserve of energy even in the dark[1,2]. These stored forms are consumed by heterotrophic organisms, providing them with carbon sources and releasing ATP during the breakdown of these compounds.

The efficient CO_2 uptake and H_2O absorption is essential, and this is facilitated by small pores on the plant surface called stomata, formed by a pair of guard cells[3-7]. Terrestrial plants have restricted these uptake openings to stomata, preventing unnecessary water loss while monitoring and adjusting for various environmental signals such as light, abiotic stresses, and biotic stresses[6,8,9]. Over time, these plants have developed highly specialized mechanisms to efficiently absorb the required CO_2 under constantly changing environmental conditions. The stomatal movements are regulated by changes in turgor pressure within the cells. The influx of K^+ ions, which act as osmotic agents, is primarily controlled by voltage-gated inward-rectifying K^+ ion channels, which are dependent on the membrane potential, making the regulation of membrane potential crucial[9]. To induce membrane hyperpolarization, the plasma membrane H^+-ATPase plays a key role[10,11].

The plasma membrane H^+-ATPase is a P-type ATPase, 10 transmembrane domain primary transporter that uses the energy from ATP hydrolysis to pump H^+ ions out of the cell, creating an electrochemical gradient across the cell membrane[12]. It is expressed throughout the plant and is essential for plant survival[12-15]. The cytoplasmic loops protruding from the fourth and fifth transmembrane domains contain the catalytic regions responsible for ATP hydrolysis[12,16,17]. At the N-terminal and C-terminal end within the cytoplasm, and the autoinhibitory domain of approximately 100 amino acids at the C-terminal region[12,18,19]. By interacting with the catalytic region, they inhibit hydrolysis and form an inactive state[20,21]. The C-terminal tail is regulated by phosphorylation in response to environmental signals, such as light[22]. In the case of stomatal opening in response to blue light, H^+-ATPase is activated, and biochemical analyses have detected phosphorylation of the penultimate Thr in the C-terminal region and its dependent binding with 14-3-3 proteins[22,23]. However, there remain many unresolved

questions regarding the kinase that directly phosphorylates the penultimate Thr and the overall mechanisms controlling H^+-ATPase activity. Furthermore, it is still unclear whether H^+-ATPase plays a role in stomatal opening in response to photosynthesis.

In this study, Chapter Ⅰ showed that a novel blue light-dependent phosphorylation site within the autoinhibitory domain of H^+-ATPase, Thr-881, was identified in addition to the penultimate Thr residue of H^+-ATPase by phosphoproteome analysis using guard cell protoplasts. We found that these phosphorylations need to H^+-ATPase activation and stomatal opening in response to light. Chapter Ⅱ focused on isolated *Arabidopsis thaliana* mutants that light-induced stomatal response was suppressed.

Chapter Ⅰ

Light-induced stomatal opening requires phosphorylation of the C-terminal auto-inhibitory domain of plasma membrane H^+-ATPase

Abstract

Plasma membrane H^+-ATPase provides the driving force for light-induced stomatal opening. However, the mechanisms underlying the regulation of its activity remain unclear. Here, we show that the phosphorylation of two Thr residues in the C-terminal autoinhibitory domain is crucial for H^+-ATPase activation and stomatal opening in *Arabidopsis thaliana*. Using phosphoproteome analysis, we show that blue light induces the phosphorylation of Thr- 881 within the C-terminal region I, in addition to penultimate Thr-948 in AUTOINHIBITED H^+-ATPASE 1 (AHA1). Based on site-directed mutagenesis experiments, phosphorylation of both Thr residues is essential for H^+ pumping and stomatal opening in response to blue light. Thr-948 phosphorylation is a prerequisite for Thr-881 phosphorylation by blue light. Additionally, red light- driven guard cell photosynthesis induces Thr-881 phosphorylation, possibly contributing to red light-dependent stomatal opening. Our findings provide mechanistic insights into H^+-ATPase activation that exploits the ion transport across the plasma membrane and light signalling network in guard cells.

Introduction

Stomata, i.e., tiny pores on the surface of leaves in land plants, play a vital role in plant development as well as in the regulation of gas exchange between plants and the atmosphere[3-7]. Stomata open in response to light, facilitating the uptake of CO_2 for photosynthetic carbon fixation and delivery of mineral nutrients absorbed by roots from the soil via transpiration. Light-induced stomatal opening consists of two distinct mechanisms, namely red and blue light responses, and these stimuli increase turgor pressure within a pair of guard cells, thus inducing stomatal opening[10,11,24]. The red light response relies on photosynthesis and requires a high intensity of red light, whereas the blue light-specific response can be induced by a low intensity of blue light triggered by receptor kinase phototropins. The blue light response is enhanced depending on the background red light intensity, and the stomatal aperture illuminated simultaneously with blue and red light is larger than the sum of the apertures illuminated with blue and red light alone[10,24]. Such a synergistic effect of blue and red light on stomatal opening is partially explained by the interaction of phototropin-mediated responses with responses caused by the reduction in intercellular CO_2 concentration (*Ci*) in leaves through photosynthetic CO_2 assimilation[25-28].

Phototropins (phot1 and phot2) are plant-specific blue light receptors comprising two photosensory light, oxygen, or voltage (LOV) domains at the N-terminus and a Ser/Thr kinase domain at the C-terminus[29,30]. Blue light perception by LOV domains activates their kinase domain and undergoes autophosphorylation at the Ser residues in the kinase activation loop, which is a prerequisite for phototropin-mediated responses, including stomatal opening, phototropism, chloroplast movements, and leaf expansion[30,31]. Phototropins phosphorylate their downstream substrates to convert and transmit light signals into intracellular signals, thereby inducing various physiological responses. Genetic and biochemical studies have identified BLUE LIGHT SIGNALING1 (BLUS1), a guard cell-specific Ser/Thr protein kinase essential for blue light-dependent stomatal opening[32]. Phototropins physically interact with BLUS1 and phosphorylate Ser-348 in the C-terminal regulatory domain of BLUS1 in a blue light-dependent manner, which abates autoinhibition of the kinase domain[28,32,33]. Activated BLUS1 transduces signals through downstream components, such as the group C1 Raf-like MAP kinase kinase kinase (MAPKKK) BLUE LIGHT-DEPENDENT H^+-ATPASE PHOSPHORYLATION (BHP) and type 1 protein phosphatase (PP1), ultimately activating plasma membrane H^+-ATPase[34-36]. Phototropins also phosphorylate another substrate, namely the CONVERGENCE OF BLUE LIGHT AND CO_2 1 (CBC1), which is a group C7 Raf-like MAPKKK[37]. CBC1, together with its paralogue CBC2, suppresses plasma membrane S-type anion channels via blue light[37,38]. Both blue light-dependent H^+-ATPase activation and anion channel inhibition contribute to plasma membrane hyperpolarisation, which drives K^+ uptake via voltage-gated inward-rectifying K^+ channels[9]. K^+ accumulation in the guard cells leads to water influx, resulting in increased turgor pressure and stomatal opening.

Plasma membrane H^+-ATPase is an electrogenic pump highly conserved among plants, algae, and fungi[16]. It exports cellular H^+ coupled with ATP hydrolysis, creating an electrochemical H^+ gradient across the plasma membrane, which energises the fundamental transport processes[12]. In the *Arabidopsis thaliana* genome, 11 genes encoding functional H^+-ATPase, designated *AUTOINHIBITED H^+-ATPASE 1–11* (*AHA1–AHA11*), have been identified. Owing to its physiological significance, plant H^+-ATPase is expressed in various cell types, such as guard cells, phloem companion cells, bundle-sheath cells, pollen cells, and root epidermis[13-15]. The plasma membrane H^+-ATPase has 10 transmembrane segments with cytoplasmic actuator (A), nucleotide-binding (N), and phosphorylation (P) domains responsible for catalytic activity[17]. The C-terminal peptide, composed of approximately 100 residues, functions as an autoinhibitory domain and inhibits enzyme activity by interfering with the catalytic domain[18,20,39]. Blue light induces the phosphorylation of the penultimate Thr residue of H^+-ATPase and subsequent binding of 14-3-3 proteins in guard cells[22]. Numerous studies that used a system heterologously expressing plant H^+-ATPase in a yeast strain conditionally devoid of endogenous plasma membrane H^+-ATPase *PMA1* have suggested that penultimate Thr phosphorylation and phosphorylation-dependent 14-3-3 protein binding may reverse C-terminal autoinhibition and activate H^+-ATPase[23]. However, genetic evidence regarding whether penultimate Thr phosphorylation is involved in H^+-ATPase activation in plants is lacking.

Furthermore, recent studies have shown that, in addition to the penultimate Thr, phosphorylation of the Thr residue upstream of the C-terminal autoinhibitory domain causes H^+-ATPase activation. The inhibitory effect of the C-terminal domain on H^+-ATPase activity is thought to be caused by two regions (regions I and II) which possibly interact and interfere with the catalytic domains[20,21]. The Thr-881 of AHA1 in region I is highly conserved in plants, and a recent study showed that AHA2 phosphorylation at Thr-881 is enhanced in *Arabidopsis* roots under low K^+ conditions[40]. Mutational experiments using a yeast heterologous expression system have indicated that the phosphorylation of Thr-881 increases H^+-ATPase activity without affecting 14-3-3 protein binding[41]. However, it is unclear whether Thr-881 is also phosphorylated by blue light in guard cells, and the functional significance of Thr-881 phosphorylation in plants has yet to be verified.

A previous thermal imaging analysis identified an *Arabidopsis aha1* mutant defective in stomatal opening in response to blue light[42]. The *aha1* mutant reduced the protein expression of total H^+-ATPase in guard cells to 30% that of wild-type plants, suggesting that AHA1 is the major isoform of the plasma membrane H^+-ATPase in guard cells[42]. Importantly, blue light-dependent H^+ pumping in guard cell protoplasts was significantly attenuated in the *aha1* mutant, and the expression of wild-type *AHA1* gene in the *aha1* mutant under the control of the native *AHA1* promoter restored the stomatal blue light responses[42]. Thus, guard cells from the *aha1* mutant offer a reliable system for the functional analysis of H^+-ATPase activation process in plants.

In the present study, we performed a phosphoproteome analysis using guard cell protoplasts and

found that the Thr-881 of AHA1, together with the penultimate Thr-948, was phosphorylated in response to blue light. We showed that the phosphorylation of both Thr-881 and Thr-948 is crucial for H^+-ATPase activation, which allows stomatal opening. Furthermore, we found that Thr-881 was phosphorylated by guard cell photosynthesis, which may contribute to the mechanism of red light-dependent stomatal opening in intact leaves.

Results

Blue light induces phosphorylation of AHA1 at Thr-881 and Thr-948 in the guard cells.

The guard cell protoplasts from the wild-type and *phot1-5 phot2-1* double mutant were illuminated with high-fluence-rate red light for 30 min, followed by a short pulse of blue light for 30 s superimposed on a background red light[32,37]. Trichloroacetic acid was added to the protoplasts to recover the proteins before and after blue-light irradiation, and trypsin and Lys-C were used to cleave them into peptides. The phosphopeptides were enriched from the digested samples by hydroxy acid-modified metal oxide chromatography (HAMMOC)[42] and analysed by nano-liquid chromatography tandem mass spectrometry (nanoLC/MS/MS). Phosphopeptides that were phosphorylated in response to blue light in a phototropin-dependent manner, including the phototropin substrates BLUS1 and CBC1, were identified[32,37]. In these analyses, blue light-dependent phosphorylation of the penultimate Thr residue of AHA1 (Thr-948) was also identified (Fig. Ⅰ-1a, b; ref 37). Furthermore, the phosphorylation level of AHA1 at Thr-881, located in region I within the C-terminalautoinhibitory domain, was also elevated in response to blue light (Fig. Ⅰ-1a, b). In contrast, blue light-dependent phosphorylation of both Thr-881 and Thr-948 was not detected in the *phot1-5 phot2-1* mutant (Fig. Ⅰ-1b). Antibodies recognising phosphorylated Thr-881 and Thr-948 of AHA1 were produced, and it was confirmed that both Thr residues were phosphorylated in response to blue light in the guard cells of the wild-type but not in those of the *phot1-5 phot2-1* mutant (Fig. Ⅰ-1c, d). Both Thr-881 and Thr-948 were conserved among the 11 AHA isoforms, except for AHA10, in which the amino acid residue corresponding to Thr-881 was replaced by a hydroxyl-containing Ser residue (Fig. Ⅰ-1e). In addition, blue light-dependent phosphorylation of AHA1/AHA2 at Thr-881, AHA5 at Thr-881, and AHA11 at Thr-889 corresponding to AHA1 at Thr-881 was detected (Fig. Ⅰ-2a, b). Furthermore, blue light-dependent phosphorylation of the penultimate Thr residue in AHA2 at Thr-947, AHA4/AHA11 at Thr-959/955, and AHA5/8 at Thr-948/947 was also detected[37].

Phosphorylation of both Thr-881 and Thr-948 is essential for stomatal opening and H^+-ATPase activation.

To address the physiological significance of phosphorylation of AHA1 at Thr-881 and Thr-948 in stomatal responses, transgenic plants expressing the non-phosphorylatable form of AHA1, in which either Thr-881 or Thr-948 was replaced by Ala (designated T881A or T948A) in the *aha1-9* null mutant background, were constructed. Consistent with previous reports[42], our immunoblot analysis showed that the total protein levels of H^+-ATPase in the guard cells were reduced to 30% in the *aha1-9* mutant compared with those in the wild-type (Fig. Ⅰ-3a, b). Transgenic lines with AHA1 protein levels in guard cells comparable to those in the wild-type plants were selected (Fig. Ⅰ-3a, b), and the results confirmed that the stomatal length, density, and index in these transgenic lines were not different from those in the wild-type and *aha1-9* mutant (Fig. Ⅰ-4a-c).

Light-dependent stomatal opening in the intact leaves was examined using gas exchange measurements (Fig. Ⅰ-5a–c). A high fluence rate of red light resulted in stomatal opening in the wild-type, and superimposition of a low fluence rate of blue light on the background red light elicited further stomatal opening. In contrast, the rate of stomatal opening induced by red light decreased in the *aha1-9* mutant compared to that in the wild-type (Fig. Ⅰ-5b). The *aha1-9* mutant also showed a decrease in both the rate and magnitude of stomatal opening in response to blue light (Fig. Ⅰ-5b, c). Transformation of *aha1-9* with the wild-type *AHA1* gene rescued the stomatal opening induced by red and blue light. However, the introduction of either *T881A* or *T948A* into *aha1-9* failed to restore the stomatal opening in response to red and blue light. The stomatal aperture in the isolated epidermis of phosphodefective lines was further evaluated (Fig. Ⅰ-5d). Irradiation with red and blue light increased the stomatal aperture in the wild-type and AHA1 lines, but not in the *aha1-9* mutant. The expression of T881A and T948A did not recover the stomatal opening defects of *aha1-9*.

To determine the impact of phosphodefective mutations on H^+-ATPase activation, blue light-dependent H^+ pumping in the guard cell protoplasts was measured (Fig. Ⅰ-5e, f). In the wild-type, blue light caused a decrease in the pH of the outer medium of guard cell protoplasts. Similar to stomatal opening, H^+ pumping was attenuated by blue light in the *aha1-9* mutant, as well as in the T881A and T948A lines compared with that in the wild-type and AHA1-expressing lines. Together, these findings suggested that the phosphorylation of both Thr-881 and Thr-948 by blue light is essential for stomatal opening and activation of H^+-ATPase.

Phosphorylation of Thr-881 by blue light depends on the phosphorylation state of Thr-948.

Studies have shown that phot1 and phot2 redundantly induce the phosphorylation of the penultimate Thr residue of H^+-ATPase through signalling pathways mediated by BLUS1 and PP1[32,34,44]. Therefore, we examined whether the phosphorylation of Thr-881 by blue light is mediated by a common signalling pathway with Thr-948 phosphorylation. Blue light-dependent phosphorylation of Thr-881 and Thr-948 was not detected in the *phot1 phot2* double mutant (Fig. Ⅰ-1c, d), but was observed in the *phot1* and *phot2* single mutants, although their phosphorylation was more significantly reduced in the *phot1* mutant than in the *phot2* mutant (Fig. Ⅰ-6a). Phosphorylation of Thr-881 and Thr-948 was absent in the guard cells of the *blus1* mutant (Fig. Ⅰ-6b). Furthermore, tautomycin, an inhibitor of PP1, suppressed the phosphorylation of both Thr residues in response to blue light (Fig. Ⅰ-6c).

To study the phosphorylation mechanism of Thr-881 and Thr-948 by blue light in more detail, we determined whether their phosphorylation by blue light depends on their phosphorylation state. Thr-948 phosphorylation was apparent in the T881A line as well as in the wild-type and AHA1 line (Fig. Ⅰ-6d, e). The binding of 14-3-3 proteins to the phosphorylated penultimate Thr-948 analysed by protein blotting was not affected by the T881A mutation in response to blue light (Fig. Ⅰ-7a, b). In

contrast, Thr-881 phosphorylation in the T948A line was much lower than that in the wild-type and AHA1 line (Fig. Ⅰ-6f, g). These results suggested that Thr-948 phosphorylation was a prerequisite for blue light-dependent Thr-881 phosphorylation. Consistent with these results, we observed that the phosphorylation of Thr-881 was slower than that of Thr-948 in response to blue light. We determined the phosphorylation of both Thr residues in the guard cells after blue light pulse (Fig. Ⅰ-6h, i). The phosphorylation of Thr-948 became evident 30 s after the start of the pulse; subsequently, it gradually increased and reached a maximum at 90 s. In contrast, the phosphorylation of Thr-881 was detected 60 s after blue light and reached a maximum at 90 s.

Blue light activation of H^+-ATPase requires phosphorylation of both Thr-881 and Thr-948.

To explore the impact of Thr-881 and Thr-948 phosphorylation on stomatal opening and activation of H^+-ATPase, we expressed phosphomimetic forms of AHA1 with the substitution of Thr-881 or Thr-948 with the acidic amino acids Asp (D) or Glu (E) in the *aha1-9* mutant. We verified the expression of AHA1 variants and stomatal morphology in the transgenic lines (Figs. Ⅰ-8 and 9). However, this attempt in Thr-948 was unsuccessful because the T948D and T948E lines failed to complement the stomatal opening in the *aha1-9* mutant (Fig. Ⅰ-10). Furthermore, our protein blot analysis revealed that blue light-dependent binding of 14-3-3 proteins to H^+-ATPase was abolished in the T948E variant (Fig. Ⅰ-11), implying that the T948D and T948E mutations could not adequately mimic the phosphorylation state of Thr-948. In contrast, the T881D line displayed a considerably larger stomatal aperture than that of the wild-type in the dark (Fig. Ⅰ-12a). In accordance with these results, the T881D line exhibited higher ATP hydrolysis activity than that of the wild-type, *aha1-9*, AHA1, and T881A expression lines (Fig. Ⅰ-12b). These findings suggested that the T881D mutation promotes H^+-ATPase activity.

Furthermore, we found that the T881D line, similar to the wild-type, showed blue light-dependent phosphorylation of Thr-948 (Fig. Ⅰ-12c, d). Furthermore, this line exhibited H^+ pumping in response to blue light in the guard cell protoplasts (Fig. Ⅰ-12e, f). We created transgenic lines harbouring double mutations of T881D T948A in AHA1 (Figs. Ⅰ-8 and 9) and found that H^+ pumping by blue light was abolished in the T881D T948A expressing line. Together, these results suggested that Thr-948 phosphorylation also stimulates H^+-ATPase activity and that phosphorylation of both Thr-881 and Thr-948 by blue light may ensure full activation of H^+-ATPase.

Guard cell photosynthesis mediates Thr-881 phosphorylation.

The stomatal response to red light was delayed in the T881A and T948A lines as well as in the *aha1-9* mutant (Fig. Ⅰ-13a, b). Our guard cell phosphorylation analysis showed that Thr-881 is phosphorylated in response to red light in addition to blue light. Following red light irradiation, the phosphorylation level of Thr-881 increased and was further enhanced by the superimposition of blue

light on red light (Fig. Ⅰ-13a, b). However, unlike Thr-881, Thr-948 was not phosphorylated by red light but was phosphorylated in a blue light-dependent manner.

Red light-induced phosphorylation of Thr-881 was completely inhibited after treatment with the photosynthetic electron transport inhibitor 3-(3,4-dichlorophenyl)-1, 1-dimethylurea (DCMU), suggesting that this phosphorylation relies on guard cell photosynthesis (Fig. Ⅰ-13c, d). In contrast, blue light-dependent phosphorylation of Thr-881 was not affected by the DCMU treatment (Fig. Ⅰ-13c, d, and 14). Furthermore, Thr-881 phosphorylation by red light was evident in the *phot1 phot2* and *blus1* mutants (Fig. Ⅰ-13e–h).

We further evaluated whether Thr-948 phosphorylation is required for Thr-881 phosphorylation by red light. Red light-induced Thr-881 phosphorylation was found in the T948A line as well as in the wild-type (Fig. Ⅰ-13i, j), suggesting that Thr-881 phosphorylation by red light does not require Thr-948 phosphorylation. Collectively, these findings suggested that red light-induced Thr-881 phosphorylation relies on guard cell photosynthesis and is distinct from phototropin-mediated blue light signalling.

Discussion

In this study, we demonstrated that blue light induces the phosphorylation of two Thr residues of the plasma membrane H^+-ATPase in guard cells, which is crucial for stomatal opening. The phosphoproteome analysis using guard cell protoplasts revealed that Thr-881 and Thr-948, located in the C-terminalautoinhibitory domain of AHA1, were phosphorylated in response to blue light (Fig. Ⅰ-1a, b). The immunoblot analysis using antibodies specific for individual Thr residues showed that these residues were phosphorylated in a blue light- and phototropin-dependent manner (Fig. Ⅰ-1c, d). Substitution of Thr-881 and Thr-948 in AHA1 with Ala abrogated the stomatal opening induced by blue light (Fig. Ⅰ-5a–d). Furthermore, both the T881A and T948A lines showed impairment of blue light-dependent H^+ pumping from guard cell protoplasts (Fig. Ⅰ-5e, f). These findings are consistent with the growth defects of yeast transformants bearing mutations in which the conserved Thr in region I and penultimate Thr were replaced by Ala[41,45,46]. From these results, we concluded that phosphorylation of both Thr-881 and Thr-948 of AHA1 is essential for blue light-dependent activation of H^+-ATPase in guard cells.

Numerous previous studies have reported Thr-948 phosphorylation in guard cells in response to blue light[22,47]. In this study, we discovered that Thr-881 is also phosphorylated in guard cells in both blue light- and photosynthesis-dependent manners. A recent study suggested that Thr-881 is phosphorylated in plants in response to low K^+ treatments[40]. Thus, the phosphorylation level of Thr-881 appears to be regulated as a terminal point in the signalling pathways of various external cues.

Furthermore, we examined the relationship between Thr-881 and Thr-948 phosphorylation on AHA1 in response to blue light. The time-course analysis revealed that compared to that of Thr-948, the start of phosphorylation of Thr-881 was delayed by blue light irradiation in wild-type guard cells (Fig. Ⅰ-6h, i). Furthermore, site-directed mutagenesis showed that blue light-dependent phosphorylation of Thr-948 and binding of 14-3-3 proteins were evident in lines harbouring the T881A mutation (Fig. Ⅰ-6d, e and 7). In accordance with these findings, the phosphorylation of penultimate Thr-955 of *Nicotiana tabacum* plasma membrane H^+-ATPase 2 (PMA2) was not significantly affected in tobacco BY2 cells expressing PMA2 variants in which Thr-889 corresponding to Thr-881 of AHA1 was replaced by Ala[45]. Similarly, phosphorylation of penultimate Thr-947 was observed when AHA2 with a T881A mutation was expressed in yeast cells[41]. In contrast, Thr-881 phosphorylation under blue light was significantly decreased in the AHA1 T948A line compared to that in the wild-type and AHA1 line (Fig. Ⅰ-6f, g). Taken together, our findings suggested that Thr-881 phosphorylation by blue light depends on the phosphorylation status of Thr-948.

It remains unclear whether Thr-881 phosphorylation is caused by a secondary response associated with Thr-948 phosphorylation or is directly regulated by blue light signals. Our findings indicated that Thr-881 phosphorylation depends on Thr-948 phosphorylation (Fig. Ⅰ-6f, g), suggesting the possibility that blue light signals are transmitted to Thr-948 to facilitate its phosphorylation,

subsequently leading to Thr-881 phosphorylation because of conformational changes coupled with Thr-948 phosphorylation without blue light signals. However, besides the requirement of Thr-948 phosphorylation as a prerequisite for Thr-881 phosphorylation, the possibility that Thr-881 may also undergo phosphorylation by protein kinases activated through blue light signals cannot be ruled out. Further research is needed to fully elucidate the mechanisms underlying blue light regulation of Thr-881 phosphorylation.

Our results showed that the T881D line displayed enhanced stomatal opening in epidermal tissues in the dark (Fig. Ⅰ-12a). Furthermore, the microsomal fraction isolated from the T881D line showed increased ATP hydrolytic activity (Fig. Ⅰ-12b). Such increased ATP hydrolysis activity was also observed in yeast cells expressing the phosphomimetic PMA2 T899D variant[45]. Thus, the phosphorylation of Thr-881 in AHA1 appears to promote H^+-ATPase activity. In addition, Thr-948 phosphorylation was prominent when the T881D cell line was exposed to blue light (Fig. Ⅰ-12c, d). Furthermore, the T881D line showed blue light-dependent H^+ pumping activity, whereas the blue light response in the T881D line was abrogated by introducing an additional T948A mutation (Fig. Ⅰ-12e, f). Consistent with our findings, the expression of AHA2 T881D and PMA2 T889D increased yeast growth in low-pH media, but such growth enhancement was lost in lines expressing AHA2 T881D T947A and PMA2 T889D T955A[41,45]. From these results, we concluded that the simultaneous phosphorylation of Thr-881 and Thr-948 by blue light induces full activation of H^+-ATPase.

The functional impact of Thr-881 and Thr-948 phosphorylation on H^+-ATPase activity remains unknown. Previous Ala scanning mutagenesis experiments and expression of various C-terminal truncated constructs indicated that regions I and II in the C-terminal region of H^+-ATPase play an important role in the autoinhibition of catalytic activity[48]. Treatment of the plasma membrane with trypsin removes the C-terminal segment from H^+-ATPase, resulting in the activation of H^+ pumping in the plasma membrane vesicles[18]. The synthetic peptide containing region I inhibits H^+ pumping by trypsin-activated H^+-ATPase[18], implying an interaction between region I peptide and the rest of the C-terminally truncated H^+-ATPase. Indeed, a yeast interaction assay confirmed the binding of the C-terminal region to the central loop of plasma membrane H^+-ATPase[39]. In vivo cross-linking experiments revealed inter- and intramolecular interactions of amino acids between the C-terminal and the catalytic domain of H^+-ATPase[20,49]. Furthermore, recent cryo-electron microscopy studies of yeast and *Neurospora crassa* PMA1 revealed that the C-terminal peptide, including region I, forms an α helix structure that mediates the interaction between the P-domain and the neighbouring P-domain via salt bridges in the autoinhibited state[50,51]. In contrast, the C-terminal helix becomes disordered in the active state, enabling the movement of the P-domain, which is essential for ATP catalysis[51]. The C-terminal regulatory helix of PMA1 contains three phosphorylation sites, namely Ser-899, Ser-911, and Thr-912. Although no structural information of the phosphorylated C-terminal domain is available, the structural analysis described above suggested that these phosphorylations may alleviate

autoinhibition by disrupting salt bridges and suppressing the helix from binding to the P-domain[51]. In the present study, the sequence alignment showed that Thr-881 in AHA1 is closely related to Ser-911 and Thr-912 in PMA1 (Fig. Ⅰ-1e). Therefore, phosphorylation of Thr-881 by blue light is likely to modulate the helical structure of region I and its inhibitory interactions. On the other hand, phosphorylation of the penultimate Thr residue creates a binding site, Tyr-pThr-Val, for 14-3-3 proteins[23]. Such binding of 14-3-3 proteins to the C-terminal sequence appears to cause the conversion of H^+-ATPase from a dimer to a hexamer, enhancing its activity and stabilising its activated state[21,52]. Thus, phosphorylation of Thr-881 and Thr-948 may promote H^+-ATPase activation via different modes of regulation, which is in accordance with our finding that simultaneous phosphorylation of both Thr residues is required for full activation of H^+-ATPase.

Our results indicated that Thr-881 in AHA1 is phosphorylated not only by blue light but also by red light in guard cell protoplasts. Red light-induced phosphorylation of Thr-881 was inhibited by DCMU, suggesting a requirement for guard cell photosynthesis (Fig. Ⅰ-13c, d). In contrast, no significant increase in Thr-948 phosphorylation was observed in guard cell protoplasts under red light (Fig. Ⅰ-13a, b). It has been demonstrated that red light stimulates H^+ pump activation at the plasma membrane in *Vicia faba* guard cells and that this response is inhibited by DCMU[53]. Therefore, it is plausible that red light stimulates plasma membrane H^+-ATPase by phosphorylating Thr-881 through guard cell photosynthesis.

We should note here that Thr-948 phosphorylation in the H^+-ATPase by red light differs between isolated guard cell protoplasts and guard cells in intact leaves. In guard cell protoplasts, Thr-948 phosphorylation does not occur by red light. In leaves, Thr-948 phosphorylation in guard cells was observed when the leaves were illuminated with red light[54]. This red light-induced Thr-948 phosphorylation in leaves was suppressed by DCMU[54], suggesting possible involvement of mesophyll cell photosynthesis in this process. The discrepancy in Thr-948 phosphorylation by red light between isolated protoplasts and intact leaves is probably related to the presence of diffusible signals derived from mesophyll cell photosynthesis in leaves[55]. Among the potential mesophyll signals that induce Thr-948 phosphorylation in guard cells, sucrose produced by mesophyll cell photosynthesis appears to be the most likely candidate. This idea was supported by a study showing that the exogenous application of sucrose to guard cell protoplasts induced Thr-948 phosphorylation[56]. In contrast, a recent investigation revealed that subjecting leaves to elevated CO_2 concentration resulted in Thr-948 dephosphorylation in guard cells[57]. This implies that the reduction in intercellular CO_2 concentration within leaves by mesophyll cell photosynthesis could induce Thr-948 phosphorylation in guard cells.

Importantly, red light-induced stomatal opening has been observed to be delayed in the *aha1-9* mutant[42,54], indicating that plasma membrane H^+-ATPase also plays a role in red light-induced stomatal opening, in addition to its role in blue light-dependent stomatal opening. However, direct evidence regarding the necessity of Thr-881 and Thr-948 phosphorylation in red light-induced

stomatal opening has not yet been obtained. Our data revealed that both the T881A and T948A lines showed delayed stomatal opening by red light, similar to the *aha1-9* mutant (Fig. Ⅰ-5a, b). These findings, along with other existing evidence[54], suggest that mechanisms regulating Thr-881 and Thr-948 phosphorylation in leaf guard cells by red light are distinct, with Thr-881 phosphorylation being mediated via guard cell photosynthesis and Thr-948 phosphorylation being mediated via mesophyll cell photosynthesis. Moreover, both of these phosphorylation events may contribute to the process of red light-induced stomatal opening.

Stomata open synergistically when exposed to blue light and high-intensity red light, which drives photosynthesis[10,24]. Guard cells sense the information of both blue light and photosynthetic activities and integrate it for proper control of stomatal opening. Such mechanisms are crucial for plants to ensure accurate gas exchange for photosynthetic CO_2 fixation while preventing water loss under changing light environments. Our previous findings indicated that plasma membrane hyperpolarisation, achieved by the activation of H^+-ATPase by blue light and inactivation of S-type anion channels by the decrease in intercellular CO_2 concentration via photosynthetic CO_2 fixation, acts as a key mechanism for the fine control of stomatal opening by blue and red light[28]. In addition to these mechanisms, coordinated control of the phosphorylation levels of guard cell plasma membrane H^+-ATPase by guard cell and mesophyll cell photosynthesis and blue light signals may represent a key determinant of the synergistic action of blue and red light on stomatal opening. Notably, blue light also causes dephosphorylation of guard cell H^+-ATPase, which probably functions as a negative feedback regulator of stomatal opening[28].

In this study, different phosphorylation patterns of Thr-881 and Thr-948 in guard cell protoplasts in response to blue and red light were observed. Specifically, blue light elicited phosphorylation of both Thr-881 and Thr-948, whereas red light only induced phosphorylation of Thr-881 in guard cell protoplasts (Figs. Ⅰ-1a, b and 13a, b). Mutants of *phot1 phot2* and *blus1* lost the phosphorylation of Thr-881 and Thr-948 in response to blue light, whereas they exhibited Thr-881 phosphorylation in response to red light (Figs. Ⅰ-1a–d, 3b and 13e–h). Furthermore, the T948A line exhibited impaired blue light-dependent phosphorylation of Thr-881, but it displayed red light-induced phosphorylation of Thr-881 (Figs. Ⅰ-6f, g and 13i, j). This suggests that Thr-948 phosphorylation is a prerequisite for blue light-induced Thr-881 phosphorylation but is not essential for red light-induced Thr-881 phosphorylation. Furthermore, blue light-induced Thr-881 and Thr-948 phosphorylation remained unaffected by DCMU, whereas red light-induced Thr-881 phosphorylation was inhibited by DCMU (Figs. Ⅰ-13c, d and 14)[58]. Based on these findings, we concluded that Thr-948 phosphorylation in guard cell protoplasts is regulated by phototropin-mediated blue light signalling, whereas Thr-881 phosphorylation in response to blue and red light is regulated by separate signalling pathways originating from phototropin and guard cell photosynthesis, respectively (Fig. Ⅰ-15).

The protein kinases responsible for the phosphorylation of Thr-881 and Thr-948 in response to blue

and red light remain unclear. Receptor-like transmembrane kinases (TMKs) were recently shown to be involved in auxin-induced phosphorylation of the penultimate Thr residue of H^+-ATPase[59,60]. It would be pertinent to investigate whether TMKs are responsible for Thr-881 and Thr-948 phosphorylation in guard cells in response to blue and red light. In contrast, D-clade type 2C protein phosphatases (PP2C-D) have been implicated in the dephosphorylation of the penultimate Thr[61,62]. Furthermore, the leucine-rich repeat receptor-like kinases BRI1-ASSOCIATED RECEPTOR KINASE 1 (BAK1) and PSY1-RECEPTOR (PSY1R) directly bind to and phosphorylate AHA2 at Thr-881[40,41,63]. The Thr-881 of AHA2 is phosphorylated by PLANT PEPTIDE CONTAINING SULFATED TYROSINE 1 (PSY1) in *Arabidopsis* seedlings, but not in the *psy1r* mutant[41]. In contrast, a recent study demonstrated that the phosphorylation level of AHA2 at Thr-881 is not increased by the addition of PSY1 and PSY5 to *Arabidopsis* roots[64]. Phosphorylation of Thr -881 by PSY peptides is controversial. To gain a deeper understanding of the molecular functions of Thr-881 and Thr-948 phosphorylation in light-induced stomatal opening, it is necessary to identify the protein kinases and phosphatases that regulate the phosphorylation at these critical sites in guard cells. In addition to Thr-881 and Thr-948, several phosphorylation sites in the C-terminal autoinhibitory domain that affect H^+-ATPase activity have been identified[19,65]. PROTEIN KINASE SOS2-LIKE5 (PKS5) phosphorylates AHA2 at Ser-931 and inhibits the activation of H^+-ATPase by preventing the binding of 14-3-3 proteins, regardless of the phosphorylation state of the penultimate Thr residue[66]. Similarly, phosphorylation of AHA2 at Ser-899 following the application of the peptide hormone RAPID ALKALIZATION FACTOR (RALF) results in the inactivation of H^+-ATPase via unknown mechanisms[67]. Furthermore, a recent study showed that BAK1 interacts with AHA2 and phosphorylates Ser-944, consequently stimulating AHA2 activity[63]. It would be interesting to investigate whether these sites are phosphorylated in response to other stimuli in the guard cells.

In conclusion, the present study provides insights into the molecular mechanisms underlying the light regulation of plasma membrane H^+-ATPase and stomatal opening. Considering that both Thr-881 and Thr-948 are conserved in most land plants[19], the activation of H^+-ATPase via the phosphorylation of these two Thr residues may be an evolutionarily conserved mechanism beyond light signalling in the guard cells. Elucidation of the regulatory mechanisms of Thr-881 and Thr-948 phosphorylation, using guard cells as a model case, will provide important insights into how plants control proton gradients across the plasma membrane, cytosolic pH, and cell turgor by various environmental and endogenous signals.

Materials and Methods

Plant materials and growth conditions.

In this study, *Arabidopsis thaliana* accession Col-0 and previously described mutants of *phot1-5*[68], *phot2-1*[69], *phot1-5 phot2-1*[44], *blus1-1*[32], and *aha1-9*[42] were used. The plants were grown in a mixture of soil and vermiculite (1:1) for four weeks under white light (50 μmol m^{-2} s^{-1}) with a 14/10 h light/dark cycle at 24 °C.

Phosphoproteome analysis.

Phosphoproteome analyses using guard cell protoplasts from the wild-type and *phot1-5 phot2-1* mutant were performed as described previously[32,37]. Briefly, the guard cell protoplasts were incubated under red light (600 μmol m^{-2} s^{-1}) for 30 min, after which a pulse of blue light (100 μmol m^{-2} s^{-1}, 30 s) was superimposed on the background red light (n = 3 biologically independent samples). The reaction was terminated by adding trichloroacetic acid to the protoplast suspension 2.5 min after the start of blue light illumination. The guard cell proteins were dissolved in 0.1 M Tris-HCl (pH 9.0) containing 8 M urea, protease inhibitor cocktail (Sigma) and phosphatase inhibitor cocktails 1 and 2 (Sigma). After reduction with dithiothreitol and carbamidomethylation with iodoacetamide, the samples were digested with Lys-C and trypsin, and phosphopeptides were enriched by hydroxy acid-modified metal oxide chromatography (HAMMOC) using lactic acid-modified titania[43,70]. The resulting phosphopeptides were eluted and analysed with nanoLC/MS/MS analyses (LTQ-Orbitrap, Thermo Fisher Scientific) in Data-Dependent Acquisition (DDA) mode under the following conditions.

The mass spectrometer was coupled with Ultimate3000 pump (Thermo Fisher Scientific) and an HTC-PAL autosampler (CTC Analytics). Reprosil-Pur 120 C18-AQ beads (3 μm; Dr. Maisch GmbH) packed in a self-pulled needle (150 mm length × 100 μm i.d., 6-μm opening) were used as the nanoLC column. The mobile phases consisted of 0.5% acetic acid (A) and 0.5% acetic acid and 80% acetonitrile (B). A three-step linear gradient of 5% to 10% B in 5 min, 10% to 40% B in 60 min, 40% to 100% B in 5 min, and 100% B for 10 min was applied, operating at a flow rate of 500 nL/min. A spray voltage of 2,400 V was applied. The full MS scan was acquired by Orbitrap from m/z 300 to 1,500 with a resolution of 60000. The top-10 precursor ions were selected for subsequent MS/MS scans by ion trap in the automated gain control mode, where the automated gain control values of 5.00e + 05 and 1.00e + 04 were set for full MS and MS/MS, respectively. The normalized collision-induced dissociation was set to 35.0.

Peptides and proteins were identified by database search using Mascot version 2.3 (Matrix Science) against the TAIR database (release 10) with trypsin specificity allowing up to two missed cleavages. The precursor mass tolerance and fragment ion mass tolerance were set as 3 ppm and 0.8 Da, respectively. Carbamidomethylation of cysteines was set as the fixed modification. Oxidation of methionines and phosphorylation of serines, threonines, and tyrosines were set as the variable

modifications. Peptide hits were accepted if the Mascot score was over the 95% confidence limit based on the "identity" score of each peptide and if at least three successive y- or b-ions with a further two or more y-, b-, and/or precursor-origin neutral loss ions were observed and the minimum peptide length was set to 6. A decoy database search against randomized sequences estimated less than 1% false-positive rate for the identified phosphopeptides with these criteria. Localisation of phosphorylated sites in the identified phosphopeptides was confirmed in-house Perl script to check for the presence of a site-determining ion combination[71]. The XIC peak area of the identified phosphopeptide was integrated using Mass Navigator v1.2 (Mitsui Knowledge Industry).

Generation of transgenic plants.

Transgenic plants expressing various AHA1 variants were generated as previously described with modifications[42]. The genomic sequence containing the promoter, coding region, and 3′ noncoding region of *AHA1* was amplified in two fragments using the following primers: 5'-GGCCAGTGCCAAGCTTCTACTACACATACATGAGTC-3' and 5'-GTAGCAATCAGAATTCACAAGTTGCTTCTACTGATAG-3' for the upstream sequence (5,106 bp) and 5'-CTTGATATCGAATTCCTCTATTGTAATTGATTTTGTTTAGTGAAATTG-3' and 5'-TCTAGAACTAGTGGATCCCATCCATATCTTTGGACG-3' for the downstream sequence (5,602 bp). The resulting upstream sequence was subcloned into the *Hind* III/*Eco* RI site of the pRI 101-AN vector (TaKaRa) in which the kanamycin resistance gene was replaced with the hygromycin resistance gene. The downstream sequence was subcloned into the *Eco* RI/*Bam* HI site of the pBluescript SK (+) vector (Stratagene) using the In-Fusion HD cloning kit (Clontech). The latter vector, containing the downstream sequence, was used as a template for point mutations using the QuikChange Site-Directed Mutagenesis Kit (Stratagene). The primers used were 5′-GGGCACAAGCTCAAAGGGCATTGCACGGTCTGCAGCC-3′ and 5′-GGCTGCAGACCGTGCAATGCCCTTTGAGCTTGTGCCC-3′ for T881A, 5′-GGGCACAAGCTCAAAGGGACTTGCACGGTCTGCAGCC-3′ and 5′-GGCTGCAGACCGTGCAAGTCCCTTTGAGCTTGTGCCC-3′ for T881D, 5′-GCAGGACATCACTACGCTGTGTAGTTGGAGTTGCACAACAAC-3′ and 5′-GTTGTTGTGCAACTCCAACTACACAGCGTAGTGATGTCCTGC-3′ for T948A, 5′-GCAGGACATCACTACGATGTGTAGTTGGAGTTGCACAACAAC-3′ and 5′-GTTGTTGTGCAACTCCAACTACACATCGTAGTGATGTCCTGC-3′ for T948D, and 5′-GCAGGACATCACTACGAAGTGTAGTTGGAGTTGCACAACAAC-3′ and 5′-GTTGTTGTGCAACTCCAACTACACTTCGTAGTGATGTCCTGC-3′ for T948E. After introducing mutations, the downstream sequence was amplified using the primers 5′-AGCAACTTGTGAATTCCTCTATTGTAATTGATTTTG-3′ and 5′-GTAGCAAT-CAGAATTCCATCCATATCTTTGGACGTG-3′ and inserted into the *Eco* RI site of the pRI 101-AN

vector containing the upstream sequence. The resulting constructs were transformed into the *aha1-9* mutant using *Agrobacterium tumefaciens* strain GV3101.

Isolation of guard cell protoplasts and measurement of H^+ pumping.

The guard cell protoplasts were enzymatically isolated from the fully developed leaves of 4-week-old *Arabidopsis* plants as described previously[35,47]. Blue light-dependent H^+ pumping from the guard cell protoplasts was measured using a glass pH electrode as described previously[47]. The guard cell protoplasts were incubated in 0.125 mM MES-NaOH (pH 6.0), 1 mM $CaCl_2$, 0.4 M mannitol, and 10 mM KCl under red light (300 μmol m^{-2} s^{-1}) for 2 h at 24 °C. Thereafter, a pulse of blue light (100 μmol m^{-2} s^{-1}, 30 s) was superimposed on the background red light.

Immunoblot analysis of guard cell proteins.

To determine the phosphorylation of plasma membrane H^+-ATPase, the guard cell protoplasts were incubated in 0.125 mM MES-NaOH (pH 6.0), 1 mM $CaCl_2$, 0.4 M mannitol, and 10 mM KCl under red light (300 μmol m^{-2} s^{-1}) for 30 min at 24 °C, after which a pulse of blue light (100 μmol m^{-2} s^{-1}, 30 s) was superimposed on the background red light. The reaction was terminated 3 min after the start of blue light illumination by adding trichloroacetic acid to the protoplast suspension. For tautomycin treatments, the guard cell protoplasts were preincubated under red light for 30 min, after which tautomycin was added to the final concentration of 5 μM. The protoplasts were further incubated under red light for 1 h and irradiated with a blue light pulse. For red light-induced phosphorylation of H^+-ATPase, the guard cell protoplasts were preincubated in the dark for 30 min and then illuminated under red light for 30 min. For the DCMU treatment, the guard cell protoplasts were preincubated in the dark for 10 min and further incubated in the dark for 30 min in the presence of 10 μM DCMU before red light illumination.

Immunoblotting was performed as described previously[22,35] with slight modifications. Antibodies against the plasma membrane H^+-ATPase were generated using the GST fusion protein of the hydrophilic loop of AHA1 (M320-A608) according to Kinoshita and Shimazaki (1999)[22]. Phospho-specific antibodies against Thr-881 and Thr-948 of AHA1 were generated using the synthetic peptides AQAQRpTLHGLQPKE for Thr-881 and IDTAGHHYpTV for Thr-948. Antibodies against BLUS1 have been described previously[32]. The phosphorylation of Thr-948 was also determined by protein blotting using GST-14-3-3[32,35]. Intensity of the protein bands was quantified using the ImageJ 1.48 software (National Institutes of Health).

Measurement of stomatal opening.

Stomatal conductance (g_s) of intact leaves was measured using a gas-exchange system (Li-6400; Li-Cor) under the following conditions: 350 ppm CO_2, 24 °C leaf temperature, 40–60% relative humidity,

and 200 μmol m^{-1} flow rate. The leaves of dark-adapted plants were illuminated with red light (600 μmol m^{-2} s^{-1}) for 1 h, after which blue light (10 μmol m^{-2} s^{-1}) was superimposed on the background red light for 20 min. The induction speeds ($g_{sinduction}$) of red- and blue-light-dependent stomatal opening were evaluated according to the following equation: $g_{sinduction} = (g_{st} - g_{si}) / (g_{sf} - g_{si})$[72], where g_{st} represents the values of g_s at each time point after red or blue light illumination, g_{si} represents the steady-state values of g_s before red or blue light illumination, and g_{sf} represents the maximum values of g_s under red or blue light. An approximate line was made using $g_{sinduction}$, and the time required for $g_{sinduction}$ to reach 30% of the maximum values was calculated.

For stomatal aperture measurements, the epidermis of dark-adapted plants was incubated in 5 mM MES-bistrispropane (pH 6.5), 50 mM KCl, and 0.1 mM $CaCl_2$ for 2 h in the dark or under red (50 μmol m^{-2} s^{-1}) and blue light (10 μmol m^{-2} s^{-1}). The stomatal aperture in the abaxial epidermis was observed using an inverted microscope (Eclipse TS100; Nikon) and quantified using the ImageJ 1.48 software (National Institutes of Health).

Isolation of microsomal fractions from leaves and measurement of ATP hydrolytic activity.

Microsomal fractions were isolated from the leaves and ATP hydrolytic activity was measured according to a previously described protocol with slight modifications[73]. The third or fourth leaves were homogenised with a mortar and pestle in an extraction buffer containing 50 mM MOPS-KOH (pH 7.5), 100 mM NaCl, 2.5 mM ethylenediamine-N,N,N',N'-tetraacetic acid (EDTA), 10 mM NaF, 5 mM dithiothreitol (DTT), 1 mM phenylmethylsulfonyl fluoride (PMSF), and 10 μM leupeptin. After centrifugation at 13,000 *g* for 10 min at 4 °C, the supernatants were further centrifuged at 100,000 *g* for 1 h at 4 °C, and the resulting pellet was resuspended in extraction buffer. The microsomal fractions (45 μg of protein, 100 μL) prepared as described above were mixed with an equal volume of ATPase reaction buffer containing 60 mM Tris-MES (pH 6.5), 6 mM $MgSO_4$, 100 mM KCl, 200 mM KNO_3, 1 mM ammonium molybdate, 10 μg mL^{-1} oligomycin, 0.1% (v/v) Triton X-100, 0.5 mM PMSF, and 5 μM leupeptin. To determine the ATP hydrolytic activity of the plasma membrane H^+-ATPase, the mixture was divided in half, and 2 μL of 10 mM sodium orthovanadate, an inhibitor of P-type ATPase, was added to half of the mixture. The reaction was initiated by adding 10 μL of 2 mM ATP to the mixture. The mixture was then maintained at 30 °C for 30 min, and then terminated by adding 1 mL of a stop solution containing 1.3% (w/v) SDS, 0.25% (w/v) sodium molybdate, and 0.15 M H_2SO_4. The inorganic phosphate (Pi) released via ATP hydrolysis was determined using a colorimetric method as follows: 50 μL of 1-amino-2-naphthol-4-sulfonic acid (ANSA) solution containing 0.125% (w/v) ANSA, 15% (w/v) $NaHSO_3$, and 1% (w/v) Na_2SO_4 were added to the reaction mixture, followed by incubation for 30 min at 24 °C, and the absorption at 750 nm was measured by a spectrophotometer (DU-640, Beckman). The Pi content was determined using a standard curve. The vanadate-sensitive ATP hydrolytic activity was calculated by subtracting the Pi content measured in the presence of

sodium orthovanadate from that measured in the absence of sodium orthovanadate and expressed as nmol Pi h^{-1} mg^{-1} protein.

Statistical analysis.

The data analyses carried out in this study were repeated at least three times, and the obtained values are presented as means ± standard deviations (SD). Statistical analysis was performed using the analysis of variance (ANOVA) followed by Tukey's test in Excel 2007 (Microsoft) and Excel Toukei ver. 6.05 and 8.0 (Esumi) and Student's *t*-test in Excel 2021 (Microsoft). P value thresholds were $P < 0.05$ or $P < 0.01$.

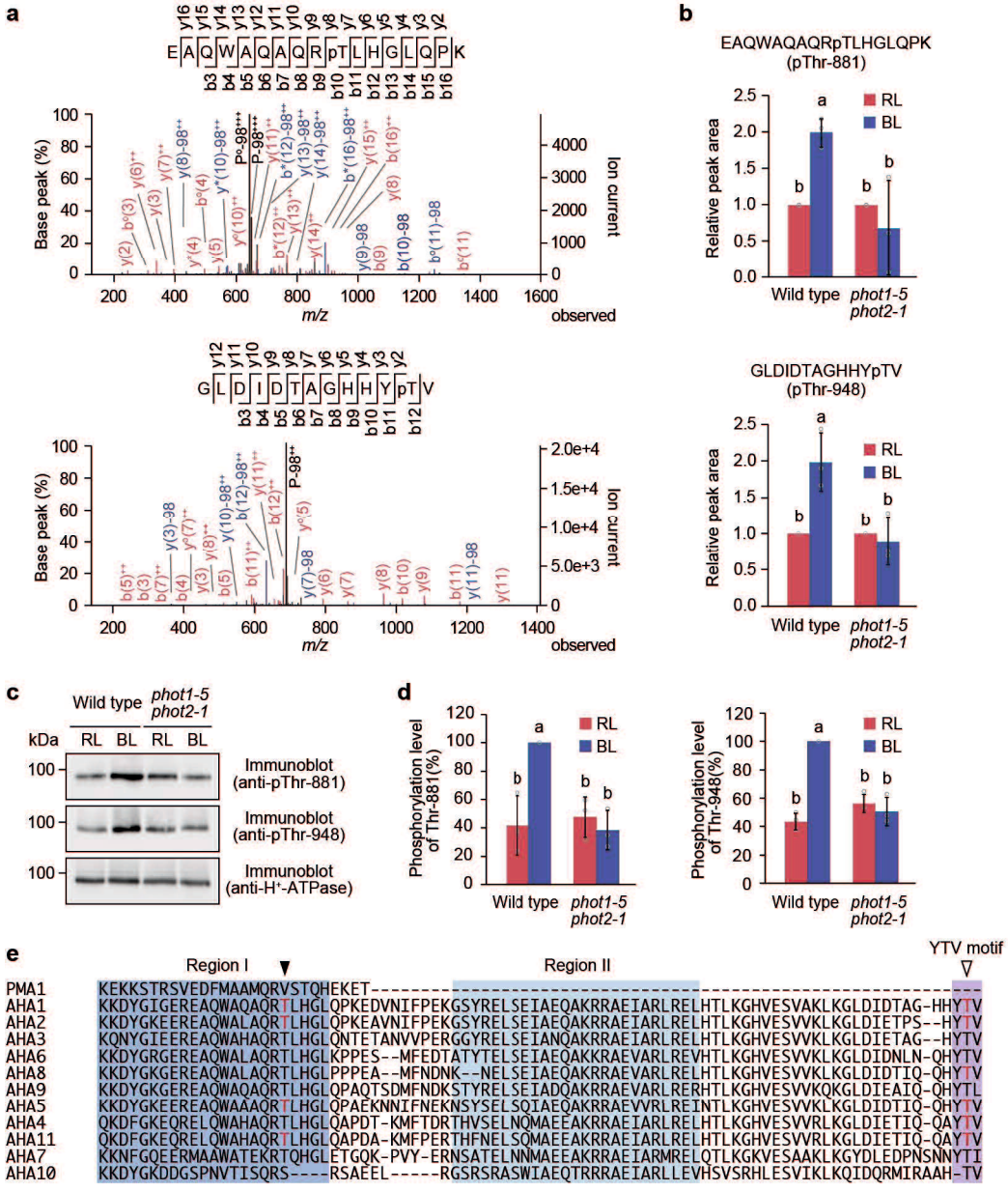
a
b
c
d
e
EAQWAQAQRpTLHGLQPK
(pThr-881)
GLDIDTAGHHYpTV
(pThr-948)
Base peak (%)
Ion current
m/z
observed
Relative peak area
RL
BL
Wild type
phot1-5
phot2-1
kDa
Immunoblot
(anti-pThr-881)
Immunoblot
(anti-pThr-948)
Immunoblot
(anti-H+-ATPase)
Phosphorylation level
of Thr-881(%)
Phosphorylation level
of Thr-948(%)
Region I
Region II
YTV motif
PMA1
AHA1
AHA2
AHA3
AHA6
AHA8
AHA9
AHA5
AHA4
AHA11
AHA7
AHA10

Fig. Ⅰ-1 Blue light-dependent phosphorylation of AHA1 at Thr-881 and Thr-948.

a, MS/MS spectra of the phosphopeptide of AHA1 containing phospho-Thr-948 and phospho-Thr-881. The labels "-98", "*", and "°" represent neutral loss of H_3PO_4, NH_3, and H_2O from b, y, and precursor (P) ions, respectively. **b,** Quantification of phosphopeptide levels calculated from integrated peak values. The data represent means ± SD (n = 3 biologically independent samples). Different letters indicate significant differences (One-way ANOVA with Tukey's test, $P < 0.05$). **c,** Phosphorylation of AHA1 at Thr-881 and Thr-948. Guard cell protoplasts were illuminated with red light (RL: 300 μmol m^{-2} s^{-1}) for 30 min, followed by a pulse of blue light (BL: 100 μmol m^{-2} s^{-1}, 30 s) superimposed on RL. The phosphorylation and amount of H^+-ATPase were detected by immunoblot analysis using anti-pThr881-AHA1, anti-pThr948-AHA1, and anti-H^+-ATPase antibodies. **d,** Relative phosphorylation levels of Thr-881 and Thr-948 were quantified using the ImageJ software. Each value is expressed as a percentage of the phosphorylation level of the wild-type under BL. Data represent means ± SD (n = 3 biologically independent samples). Different letters indicate significant differences (One-way ANOVA with Tukey's test, $P < 0.01$). **e,** Alignment of amino acid sequences of the C-terminal regulatory domain of plasma membrane H^+-ATPase in *Saccharomyces cerevisiae* (PMA1) and *Arabidopsis thaliana* (AHA1-11). Region I, Region II, and YTV motifs are highlighted in blue, light blue, and purple, respectively. The closed and open arrowheads indicate the positions of Thr-881 and Thr-948 in AHA1, respectively. The blue light-dependent phosphorylation sites identified in this study are indicated in red.

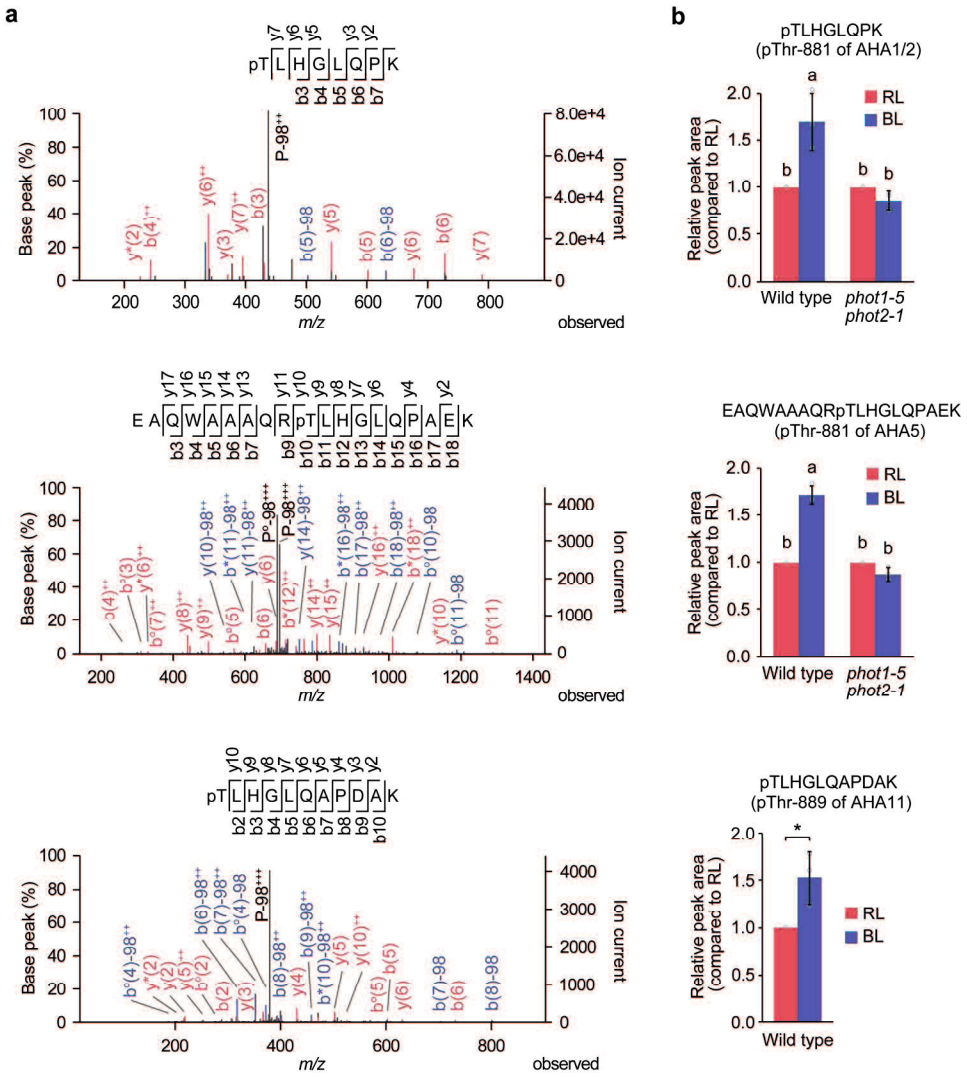

Fig. Ⅰ-2 Blue light-dependent phosphorylation of AHA proteins.

a, MS/MS spectra of AHA1/2, AHA5, and AHA11 phosphopeptides. The labels "-98", "*", and "o" represent neutral loss of H_3PO_4, NH_3, and H_2O from b, y, and precursor (P) ions, respectively. **b,** Quantification of phosphopeptide amounts calculated from integrated peak values. The data represent means ± SD (n = 3 biologically independent samples). For AHA1/2 and AHA5, different letters indicate significant differences (One-way ANOVA with Tukey's test, $P < 0.01$). For AHA11, asterisk indicates significant differences (Student's t-test, $P < 0.05$).

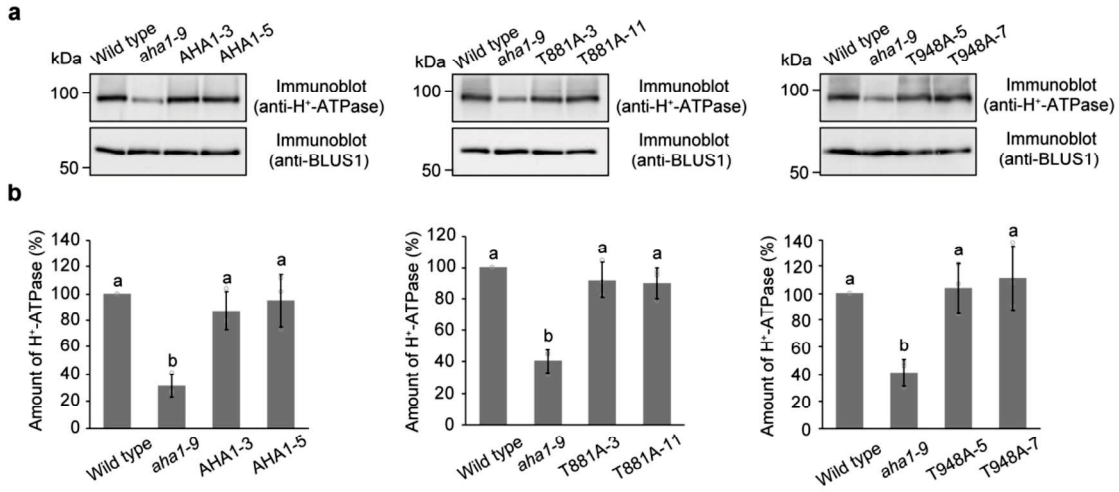

Fig. Ⅰ-3 Expression of T881A and T948A variants in the *aha1-9* background.

a, Immunoblot analysis using anti-H^+-ATPase antibodies. Each lane contains 4.2 μg of guard cell proteins. BLUS1 was used as the loading control. **b,** Quantification of the expression level of H^+-ATPase using the ImageJ software. The expression level of H^+-ATPase is expressed as a percentage of that in the wild-type. The data represent means ± SD (n = 3 biologically independent experiments). Different letters indicate significant differences (One-way ANOVA with Tukey's test, $P < 0.01$).

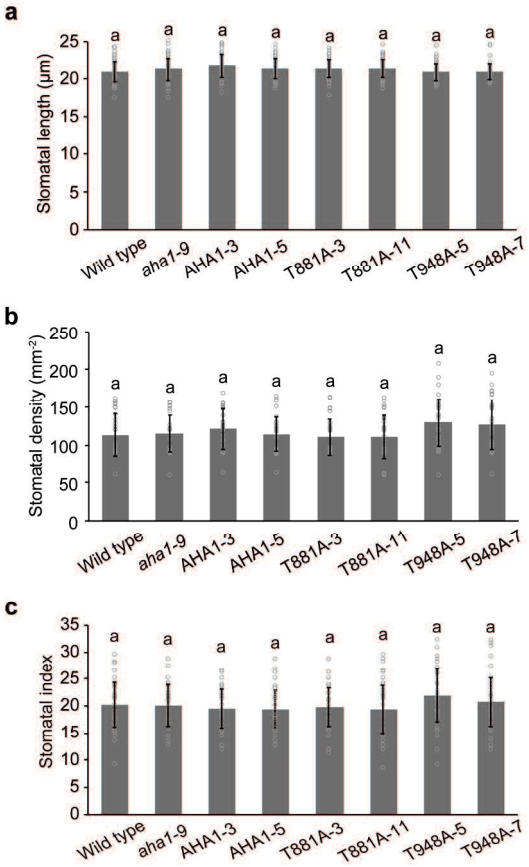

Fig. Ⅰ-4 Stomatal size, density, and index in transgenic plants expressing T881A and T948A variants. **a–c,** Stomatal size (**a**), density (**b**), and index (**c**) in the abaxial epidermis. For **(a)** and **(c)**, the data represent means ± SD (n = 60 biologically independent samples). For **(b)**, the data represent means ± SD (n = 36 biologically independent samples). Different letters indicate significant differences (One-way ANOVA with Tukey's test, $P < 0.01$).

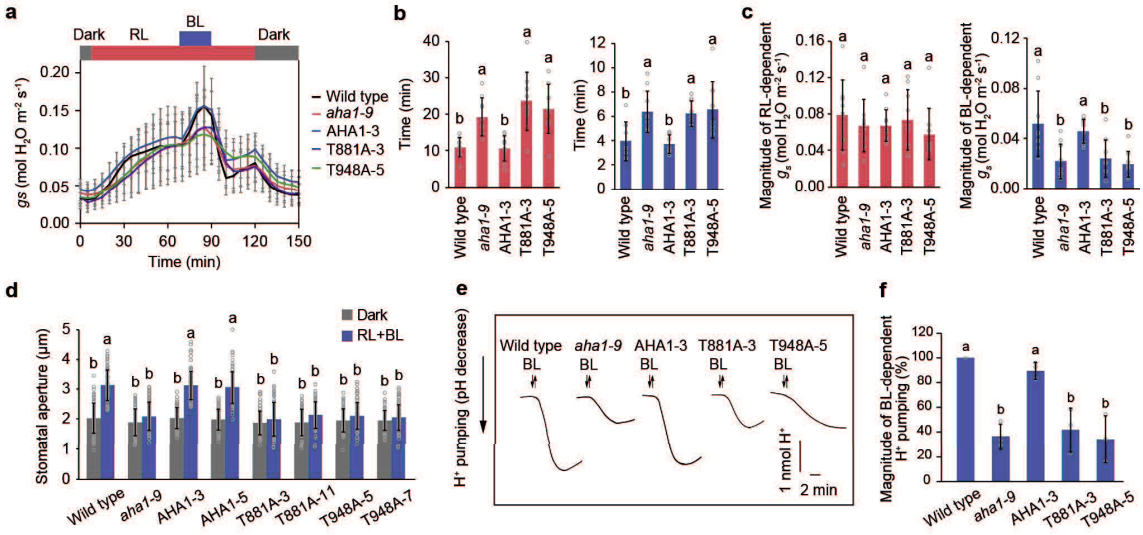

Fig. Ⅰ-5 Impairments of blue light-dependent stomatal opening and H^+ pumping in phosphodefective mutants of Thr-881 and Thr-948 of AHA1.

a, Light-dependent changes in stomatal conductance in the intact leaves. Leaves of dark-adapted plants were illuminated with red light (RL: 600 μmol m^{-2} s^{-1}) for 1 h, after which blue light (BL: 10 μmol m^{-2} s^{-1}) was superimposed on RL for 20 min. The data represent means ± SD (n = 9 biologically independent plants). **b,** Time taken to reach 30% of the maximum values of stomatal conductance in response to RL and BL. The data represent means ± SD (n = 9 biologically independent plants). Different letters indicate significant differences (One-way ANOVA with Tukey's test, $P < 0.05$). **c,** Quantification of stomatal conductance changes in response to RL and BL. The data represent means ± SD (n = 9 biologically independent plants). Different letters indicate significant differences (One-way ANOVA with Tukey's test, $P < 0.05$). **d,** Light-dependent stomatal opening. Epidermal strips were incubated in the dark or under RL (50 μmol m^{-2} s^{-1}) with BL (10 μmol m^{-2} s^{-1}) for 2 h. The data represent means ± SD (n = 75 stomata from three independent experiments). Different letters indicate significant differences (One-way ANOVA with Tukey's test, $P < 0.01$). **e,** Blue light-dependent H^+ pumping. Guard cell protoplasts were illuminated with RL (300 μmol m^{-2} s^{-1}) for 2 h, after which a BL pulse (100 μmol m^{-2} s^{-1}, 30 s) was superimposed. **f,** Quantification of the magnitude of H^+ pumping. The data represent means ± SD (n = 3 biologically independent experiments). Different letters indicate significant differences (One-way ANOVA with Tukey's test, $P < 0.01$).

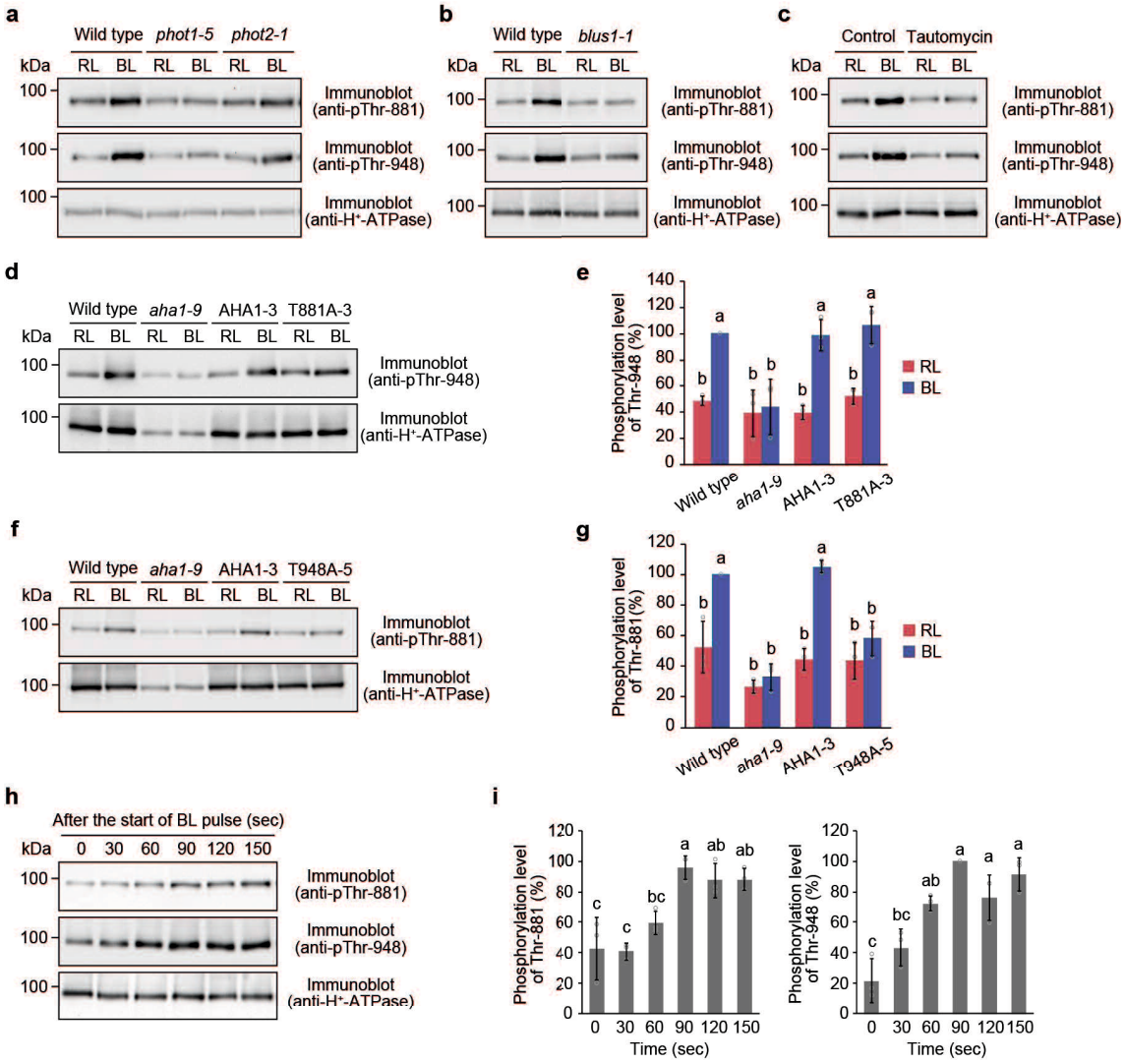

Fig. Ⅰ-6 Biochemical analysis of Thr-881 and Thr-948 phosphorylation in response to blue light. **a, b,** Phosphorylation of Thr-881 and Thr-948 in *phot1-5*, *phot2-1* (**a**), and *blus1-1* mutants (**b**). Guard cell protoplasts were illuminated with red light (RL: 300 μmol m^{-2} s^{-1}) for 30 min, after which a pulse of blue light (BL: 100 μmol m^{-2} s^{-1}, 30 s) was superimposed on the RL. The reaction was terminated 3 min after the BL pulse. **c,** Effect of the PP1 inhibitor tautomycin on Thr-881 phosphorylation. Guard cell protoplasts were pre-treated with tautomycin (5 μM) under RL for 1 h. For (**a**), (**b**), and (**c**), the experiments conducted three times on different occasions gave similar results. **d, e,** Phosphorylation of Thr-948 in the T881A mutants. **f, g,** Phosphorylation of Thr-881 in the T948A mutants. **h, i,** Time course of Thr-881 and Thr-948 phosphorylations following a BL pulse. The reaction was terminated at the indicated time points. For (**e**), (**g**), and (**i**), the relative phosphorylation levels of Thr-881 and Thr-948 were quantified using the ImageJ software. The data represent means ± SD ($n = 3$ biologically independent experiments). Different letters indicate significant differences (One-way ANOVA with Tukey's test, $P < 0.01$). For (**e**) and (**g**), each value is expressed as a percentage of the phosphorylation

level of the wild-type under BL. For (**i**), each value is expressed as a percentage of the maximum phosphorylation observed for each phospho-site in response to BL.

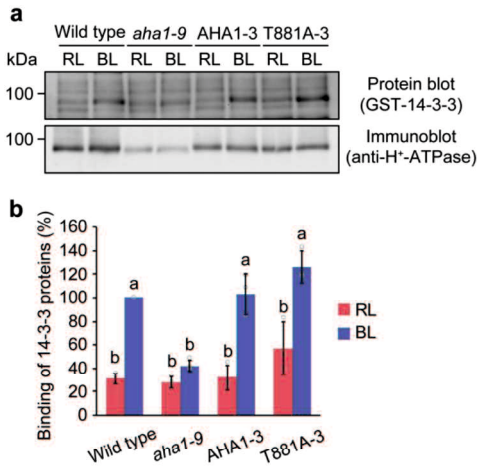

Fig. Ⅰ-7 Binding of 14-3-3 proteins to H^+-ATPase.

a, Guard cell protoplasts were illuminated with red light (RL: 300 μmol m^{-2} s^{-1}) for 30 min, after which a pulse of blue light (BL: 100 μmol m^{-2} s^{-1}, 30 s) was superimposed on RL. Binding of 14-3-3 proteins to H^+-ATPase was detected by protein blot analysis using GST-14-3-3 as a probe. **b,** Relative binding of 14-3-3 proteins to H^+-ATPase was quantified using the ImageJ software. Each binding level was expressed as a percentage of that in the wild-type under BL. The data represent means ± SD ($n = 3$ biologically independent experiments). Different letters indicate significant differences (One-way ANOVA with Tukey's test, $P < 0.01$).

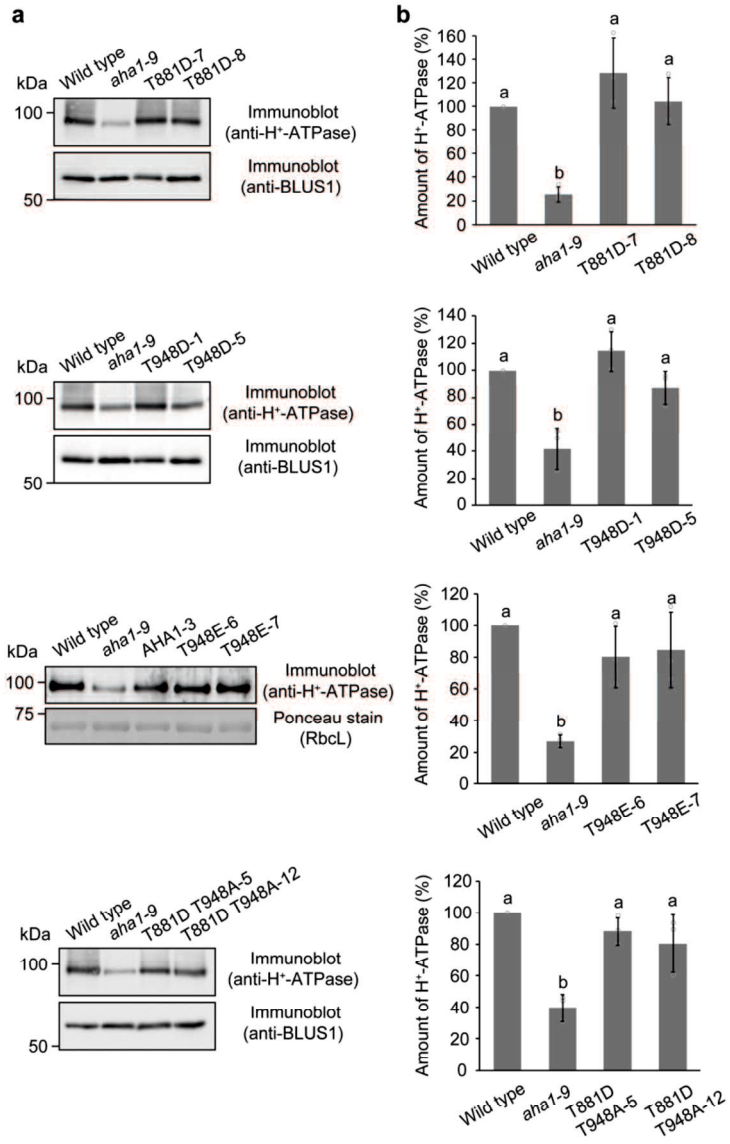

Fig. Ⅰ-8 Expression of T881D, T948D, T948E, and T881A T948A variants in the *aha1-9* background. **a,** Immunoblot analysis using anti-H^+-ATPase antibodies. Each lane contained 4.2 μg of guard cell proteins. BLUS1 and RbcL were used as loading controls. **b,** Quantification of the expression level of H^+-ATPase using the ImageJ software. The expression level of H^+-ATPase was expressed as a percentage of that in the wild-type. The data represent means ± SD (n = 3 biologically independent experiments). Different letters indicate significant differences (One-way ANOVA with Tukey's test, $P < 0.05$).

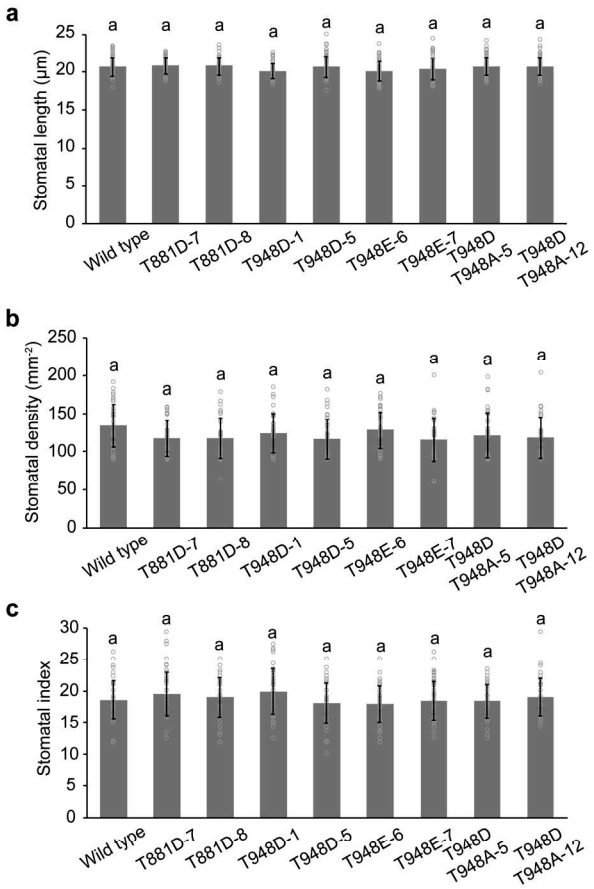

Fig. Ⅰ-9 Stomatal size, density, and index in transgenic plants expressing T881D, T948D, T948E, and T881D T948A variants.

a-c, Stomatal size (**a**), density (**b**), and index (**c**) in the abaxial epidermis. For **(a)** and **(c)**, the data represent means ± SD (n = 60 biologically independent samples). For **(b)**, the data represent means ± SD (n = 36 biologically independent samples). Different letters indicate significant differences (One-way ANOVA with Tukey's test, $P < 0.01$).

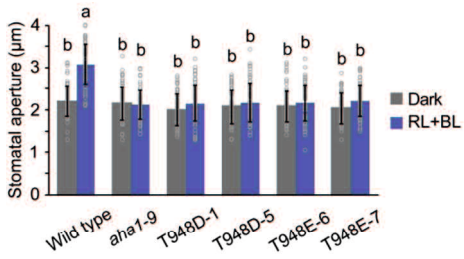

Fig. Ⅰ-10 Light-dependent stomatal opening in transgenic plants expressing T948D and T948E variants.

Epidermal strips were incubated in the dark or under red light (RL; 50 μmol m^{-2} s^{-1}) with blue light (BL; 10 μmol m^{-2} s^{-1}) for 2 h. The data represent means ± SD (n = 75 stomata from three independent experiments). Different letters indicate significant differences (One-way ANOVA with Tukey's test, $P < 0.01$).

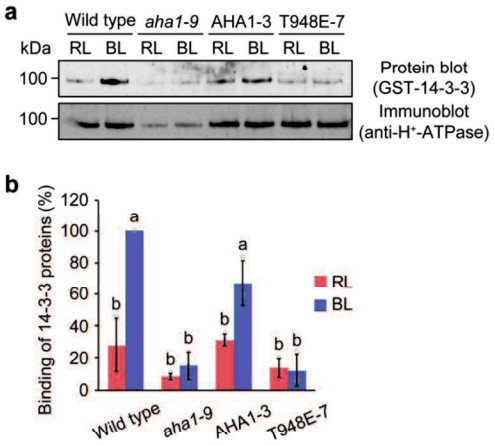

Fig. Ⅰ-11 Impairment of the binding of 14-3-3 proteins to T948E variants.

a, Guard cell protoplasts were illuminated with red light (RL: 600 μmol m^{-2} s^{-1}) for 30 min, after which a pulse of blue light (BL: 100 μmol m^{-2} s^{-1}, 30 s) was superimposed on RL. Binding of 14-3-3 proteins to H^+-ATPase was detected by protein blot analysis using GST-14-3-3 as a probe. **b,** Relative binding of 14-3-3 proteins to H^+-ATPase was quantified using the ImageJ software. Each binding level was expressed as a percentage of that in the wild-type under BL. The data represent means ± SD (n = 3 biologically independent experiments). Different letters indicate significant differences (One-way ANOVA with Tukey's test, P < 0.01).

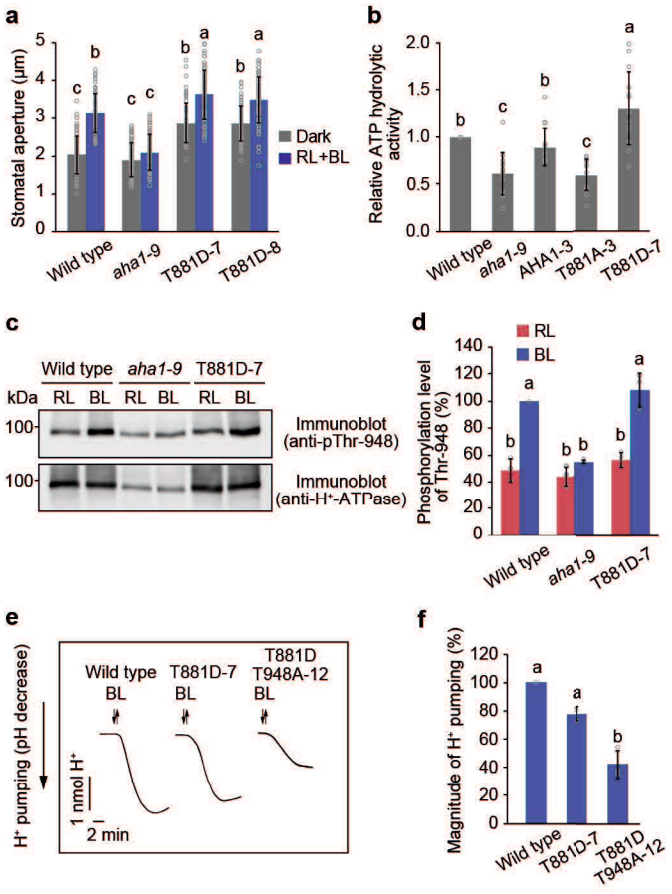

Fig. Ⅰ-12 Phosphomimetic mutation of Thr-881 enhances H^+-ATPase activity.

a, Light-dependent stomatal opening. Epidermal strips were incubated in the dark or under red light (RL: 50 μmol m^{-2} s^{-1}) with blue light (BL: 10 μmol m^{-2} s^{-1}) for 2 h. The data represent means ± SD (n = 75 stomata from three independent experiments). Different letters indicate significant differences (One-way ANOVA with Tukey's test, $P < 0.01$). **b,** ATP hydrolytic activity in the microsomal membrane fraction obtained from leaves. The data represent means ± SD (n = 14 biologically independent experiments). Different letters indicate significant differences (One-way ANOVA with Tukey's test, $P < 0.05$). **c,** Phosphorylation of Thr-948 in the T881D line. Guard cell protoplasts were illuminated with RL (300 μmol m^{-2} s^{-1}) for 30 min, after which a pulse of BL (100 μmol m^{-2} s^{-1}, 30 s) was superimposed. **d,** Relative phosphorylation levels of Thr-948 were quantified using the ImageJ software. Each value is expressed as a percentage of the phosphorylation level of the wild-type under BL. The data represent means ± SD (n = 3 biologically independent experiments). Different letters indicate significant differences (One-way ANOVA with Tukey's test, $P < 0.01$). **e,** BL-dependent H^+ pumping. Guard cell protoplasts were illuminated with RL (300 μmol m^{-2} s^{-1}) for 2 h, after which a BL pulse (100 μmol m^{-2} s^{-1}, 30 s) was superimposed. **f,** Quantification of the magnitude of H^+ pumping. The data represent means ± SD (n = 3 biologically independent experiments). Different letters indicate significant differences (One-way ANOVA with Tukey's test, $P < 0.01$).

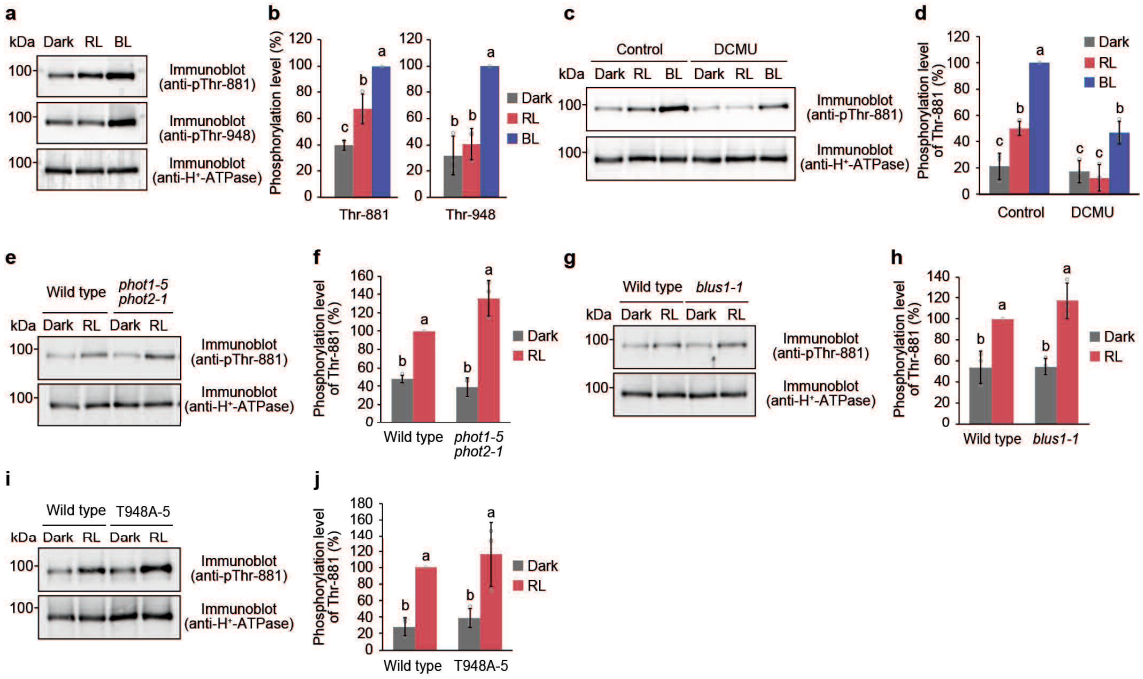

Fig. Ⅰ-13 Guard cell photosynthesis induces Thr-881 phosphorylation.

a, b, Red light-dependent phosphorylation of Thr-881. Guard cell protoplasts were incubated in the dark for 30 min or illuminated with red light (RL: 300 μmol m^{-2} s^{-1}) for 30 min, after which a pulse of blue light (BL: 100 μmol m^{-2} s^{-1}, 30 s) was superimposed on RL. **c, d,** Effect of the photosynthesis inhibitor 3-(3,4-dichlorophenyl)-1, 1-dimethylurea (DCMU) on Thr-881 phosphorylation. Guard cell protoplasts were pre-treated with DCMU (10 μM) in the dark for 30 min. **e–j,** Red light-dependent phosphorylation of Thr-881 in the *phot1-5 phot2-1* (**e, f**), *blus1-1* (**g, h**), and the T948A line (**i, j**). For (**b**), (**d**), (**f**), (**h**), and (**j**), the relative phosphorylation levels of Thr-881 and Thr-948 were quantified using the ImageJ software. The data represent means ± SD (n = 3 biologically independent experiments). Different letters indicate significant differences, One-way ANOVA with Tukey's test, $P < 0.01$ for (**b**), (**f**), and (**h**) and $P < 0.05$ for (**d**) and (**j**).

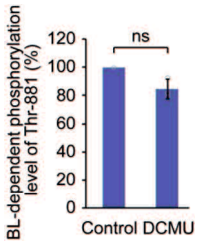

Fig. Ⅰ-14 Quantification of blue light-dependent phosphorylation of Thr-881 in the presence or absence of DCMU.

Guard cell protoplasts were pre-treated with DCMU (10 μM) in the dark for 30 min, then illuminated with red light (RL: 300 μmol m^{-2} s^{-1}) for 30 min, after which a pulse of blue light (BL: 100 μmol m^{-2} s^{-1}, 30 s) was superimposed on RL. Phosphorylation levels of Thr-881 (Fig. 5c) were quantified using the ImageJ software. Blue light-dependent phosphorylation of Thr-881 was calculated by subtracting the phosphorylation levels under red light from those under blue light and expressed as a percentage relative to control. The data represent means ± SD (n = 3 biologically independent experiments). ns indicates no significant difference ($P < 0.01$; Student's t-test).

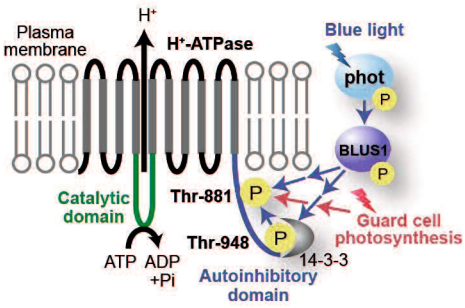

Fig. Ⅰ-15 Schematic model for blue light and photosynthesis-mediated activation of H^+-ATPase in the guard cells.

Blue light-activated phototropins phosphorylate BLUS1 protein kinase, which mediates the phosphorylation of Thr-881 and Thr-948. Thr-948 phosphorylation is a prerequisite for Thr-881 phosphorylation in response to blue light. Simultaneous phosphorylation of Thr-881 and Thr-948 promotes H^+-ATPase activity and stomatal opening. Guard cell photosynthesis also mediates Thr-881 phosphorylation.

Chapter Ⅱ

Isolation and characterization of the G26-51 mutant impaired in light-responsive activation of plasma membrane H^+-ATPase

Abstract

Phototropins activate plasma membrane H^+-ATPase, leading to hyperpolarization of the plasma membrane and creating the driving force for stomatal opening. The H^+-ATPase has cytoplasmic catalytic regions responsible for ATP hydrolysis, and its activation is regulated by a C-terminal autoinhibitory domain. Recently, our research has shown that blue light activates H^+-ATPase by phosphorylating two Thr residues, Thr-881 and Thr-948, within the autoinhibitory domain. However, the signaling pathway that connects phototropins to H^+-ATPase activation remains unclear. In this study, we isolated an *Arabidopsis* mutant, named G26-51, which is specifically impaired in blue light-dependent stomatal opening, as revealed by thermal imaging. This mutant exhibited defects in the phosphorylation of Thr-881 and Thr-948 by blue light. Additionally, the G26-51 mutant showed inhibited phosphorylation and activation of H^+-ATPase in response to fusicoccin, an H^+-ATPase activator, and red light. These findings suggest that the G26-51 mutant has impairments in the peripheral process of H^+-ATPase activation in response to light.

Introduction

Plants regulate their growth by sensing surrounding environment conditions and responding to these signals. Stomata, located on the leaf surface, facilitate CO_2 uptake for photosynthesis and enable nutrient uptake from the soil via water transport through the roots[3-7]. Stomatal aperture is regulated by various environmental signals, specifically light-induced stomatal opening involves two distinct mechanisms: the red light response, in which strong red light drives photosynthesis, and the blue light response, where weak blue light acts as a signaling cue[10,11,24]. These responses work synergistically to efficiently open stomata[10,24,28]. Photosynthesis-dependent stomatal opening has been suggested that it is driven by a decrease in intercellular CO_2 concentration (Ci) and metabolite of sugar by mesophyll chloroplasts and provisioning of ATP from guard cell chloroplasts[10,25-27,58].

In contrast, blue light-induced stomatal opening is initiated by light perception owing to photoreceptor kinase phototropins, phot1 and phot2[44]. Phototropins are comprise of two light, oxygen, or voltage (LOV) domains at the N-terminus for blue light recognition and a Ser/Thr kinase domain at the C-terminus[29,30]. Phototropins exposed to blue light allow to activate their kinase domain and transmit light signal to BLUE LIGHT SIGNALING 1 (BLUS1)[31,32]. BLUS1 topical expressed in guard cell is able to blue light-dependent stomatal opening effectively[32]. The activated phototropins phosphorylate Ser-348 in the C-terminal regulatory domain of BLUS1 and that leads to release block of own activity of Ser/Thr kinase domain in N-terminus[28,32,33]. BLUS1 transduce the signal through phosphorylation to downstream and this signal mediated by the group C1 Raf-like MAP kinase kinase kinase (MAPKKK) BLUE LIGHT-DEPENDENT H^+-ATPASE PHOSPHORYLATION (BHP) and type 1 protein phosphatase (PP1) to motive plasma membrane H^+-ATPase activation[34-36]. Another phototropins substrate has identified as the CONVERGENCE OF BLUE LIGHT AND CO_2 1 (CBC1), which is a group C7 Raf-like MAPKKK21. CBC1, along with its paralogue CBC2, suppresses plasma membrane S-type anion channels in response to blue light[37,38]. In coordinated these manners, hyperpolarization arises across the plasma membrane, which facilitate the uptake of K^+ via voltage-gated inward rectifying K^+ channel and stomatal opening as a result[9].

Plasma membrane H^+-ATPase is the pump, exporting cellular H^+ in exchange for ATP hydrolysis to create an electrochemical gradient across the plasma membrane, regulating secondary transporters for ions, amino acids, sugars, and voltage-dependent channels, thus supporting plant development[12,16,19,22]. In *Arabidopsis thaliana*, it has 11 genes encoding functional H^+-ATPase, *AUTOINHIBITED H^+-ATPASE 1–11* (*AHA1–AHA11*). H^+-ATPase is expressed in various cell types, including guard cells, root epidermal cells, phloem companion cells, bundle-sheath cells and pollen cells[13-15]. H^+-ATPase belongs to the P-type ATPase family and has ten transmembrane domains, with intracellular N- and C-terminal regions. The catalytic domain, responsible for ATP hydrolysis, is located between the fourth and fifth transmembrane regions[17,19]. This catalytic activity is tightly regulated by a C-terminal autoinhibitory domain[18].

Recently, it has been revealed that blue light signals phosphorylate the two Thr, Thr-881 and Thr-948, in the autoinhibitory domain of H^+-ATPase. Both phosphorylations are essential for blue light-dependent H^+-ATPase activation in guard cells[74,75]. Additionally, Thr-881 is phosphorylated in response to photosynthesis, contributing to rapid stomatal opening[74,75]. However, the molecular mechanisms of light-induced H^+-ATPase activation remain unclear.

To address this, we conducted *Arabidopsis* mutants screening using infrared thermography to visualize stomatal opening, inferred from the reduction in leaf temperature caused by transpiration. This screening has identified BLUS1, AHA1 that the main isoform of H^+-ATPase in guard cells, and ATG2 which plays a role in maintaining ROS homeostasis via autophagy until now[32,42,76]. This approach is expected to identify novel key factors involved in stomatal opening and we isolated the G26-51 mutant, which exhibits inhibited stomatal opening in response to blue light and lacks H^+-ATPase activation.

Results

G26-51 mutant shows inhibition of blue light response.

To identify key factors and mechanisms involved in blue light-dependent stomatal opening, we screened Ethyl methanesulfonate-treated mutants of *Arabidopsis thaliana* using thermal imaging[32]. After dark adaptation, plants were exposed to red light (100 μmol m^{-2} s^{-1}) for 50 minutes to saturate photosynthesis, followed by weak blue light (10 μmol m^{-2} s^{-1}) for 30 minutes. Thermal images taken before and after blue light exposure allowed us to visualize stomatal opening via transpirational water loss. In wild-type plants, leaf temperature decreased in response to blue light however, *phot1 phot2* double mutant did not this response (Fig. Ⅱ-1a). Like phot double mutant, isolated G26-51 mutant exhibited inhibition of this decrease leaf temperature (Fig. Ⅱ-1a). Continuous monitoring of whole leaf temperature every 30 seconds showed that the G26-51 mutant also had a slower rate of temperature decrease (Fig. Ⅱ-1b). To assess stomatal responses more directly, we measured stomatal aperture that was incubated under dark or red and blue light conditions. Consistent with the thermal imaging results, G26-51 lacked the light-induced stomatal opening seen in wild-type plants (Fig. Ⅱ-1c).

Reduced H^+-ATPase activation in the G26-51 mutant.

The G26-51 mutant displayed inhibition of blue light-dependent stomatal opening. To investigate whether this inhibition was due to reduced H^+-ATPase activation, we examined H^+ pumping via H^+-ATPase activation in guard cell protoplasts under blue light (Fig. Ⅱ-2a). In the wild-type, H^+ pumping occurred rapidly in response to a blue light pulse; however, in the G26-51 mutant, both the magnitude and maximum rate of H^+ pumping were reduced (Fig. Ⅱ-2a, b). These findings indicate that G26-51 participates in blue light-dependent stomatal opening and H^+-ATPase activation. Activation of H^+-ATPase requires phototropins and BLUS1 kinase activation[31,32]. We performed immunoblot analysis and confirmed the upstream components of blue light signaling in G26-51 (Fig. Ⅱ-2c, d). Oppositely, Thr-881 and Thr-948 of H^+-ATPase were not phosphorylated completely in this mutant (Fig. Ⅱ-2e-g).

Inhibition of Fc-induced phosphorylation of H^+-ATPase in the G26-51 mutant.

Fusicoccin (Fc), an activator of H^+-ATPase, promotes phosphorylation of the penultimate Thr, leading to irreversible phosphorylation and subsequent binding to 14-3-3 proteins. Based on previous results, it is suggested that in the G26-51 mutant, the signaling pathway leading to H^+-ATPase phosphorylation downstream of BLUS1 kinase is disrupted. If the mutation is close to the phosphorylation step of H^+-ATPase, the addition of Fc would not see phosphorylation of the penultimate Thr. To test this hypothesis, we added 10 μM Fc to guard cell protoplasts. In wild-type, Fc-induced significant phosphorylation of Thr-948, but this response was suppressed in G26-51

mutant (Fig. Ⅱ-3a). Consistent with this suppression, G26-51 mutant also showed reduced stomatal opening and H^+ pumping in response to Fc (Fig. Ⅱ-3b-d). These results suggest that the G26-51 mutant has a defect in the phosphorylation process of H^+-ATPase.

Photosynthesis induced stomatal opening in G26-51 mutant.

Phosphorylation of Thr-881 in H^+-ATPase is also involved in the rapid stomatal opening induced by photosynthesis. Therefore, we examined photosynthesis induced phosphorylation of Thr-881 in the G26-51 mutant (Fig. Ⅱ-4a, b). We observed a reduction of phosphorylation of Thr-881 and the associated rapidly stomatal response at least (Fig. Ⅱ-4a-d). These results indicate that the G26-51 mutant has reduced stomatal opening due to the absence of photosynthesis-dependent H^+-ATPase phosphorylation.

Unchanged localization of H^+-ATPase in the G26-51 mutant.

Phosphorylation of H^+-ATPase requires correct localization within the plasma membrane. To investigate this, we conducted cell fractionation using leaf samples. First, the total extraction obtained by homogenizing leaves with extraction buffer. Next, the extraction was ultracentrifuged, and the resulting pellet was resuspended in extraction buffer as the microsome fraction, while the supernatant was designated as the soluble fraction. As a control, phototropin, a membrane-bound protein, was not observed in the soluble fractions but was observed in the microsome fractions. (Fig. Ⅱ-5a). H^+-ATPase was present in the microsome fractions, but was not detected in the soluble fractions, with no difference in quantity observed between the wild-type and G26-51 mutant (Fig. Ⅱ-5a, b).

Discussion

In his study isolated an EMS-induced mutant, G26-51, from a forward genetic screen. This mutant exhibited impaired blue light-dependent stomatal opening and suggested a role in H^+-ATPase activation. Previous studies have indicated that blue light-induced H^+-ATPase activation requires phosphorylation of Thr-881 and Thr-948 within its C-terminal autoinhibitory domain[74,75]. However, the factors directly mediating this phosphorylation remained unknown. In G26-51, both Thr-881 and Thr-948 failed to be phosphorylated in response to blue light (Fig. Ⅱ-2e-g), indicating a deficiency in blue light-dependent plasma membrane H^+-ATPase phosphorylation.

G26-51 also exhibited impaired red light-induced stomatal opening (Fig. Ⅱ-4c, d). Previous work demonstrated that the *aha1-9* mutant, which has reduced H^+-ATPase levels, and phosphorylation-deficient mutants T881A and T948A, showed delayed photosynthesis-induced stomatal opening compared to wild-type[42,54,74,75]. Similarly, G26-51 exhibited impaired photosynthesis-induced Thr-881 phosphorylation in guard cells (Fig. Ⅱ-4a), indicating its involvement in both blue and red light-dependent stomatal opening via H^+-ATPase activation.

Analysis of Thr-881 and Thr-948 phosphorylation in G26-51 revealed normal phototropin autophosphorylation and BLUS1 Ser-348 phosphorylation (Fig. Ⅱ-2c, d), demonstrating normal phototropin and BLUS1 kinase activity. However, while the *phot1 phot2* double mutant and *blus1* mutants still exhibited Fc-induced Thr-948 phosphorylation (Fig. Ⅱ-3a; refs. 32, 43), this phosphorylation was reduced in G26-51. These data suggest that G26-51 has a specific impairment in the steady-state phosphorylation of Thr-948, possibly affecting the phosphorylation process.

In *Arabidopsis thaliana*, all 11 functional H^+-ATPase isoforms are expressed in guard cells, with AHA1 comprising approximately 60% of the total[42]. The *aha1-9* null mutant exhibits significantly inhibited H^+-ATPase activation[42]. G26-51 also displayed impaired H^+-ATPase activation, comparable to *aha1-9*, without a reduction in total H^+-ATPase levels in leaves (Fig. Ⅱ-2a, 4a, and 5). This suggests that G26-51 affects the activation step rather than H^+-ATPase expression. Cell fractionation studies using leaves localized H^+-ATPase in G26-51 to the microsomal fraction, similar to wild-type, though further investigation is required to confirm plasma membrane localization.

Blue light induces initial Thr-948 phosphorylation followed by Thr-881 phosphorylation, whereas photosynthesis-dependent phosphorylation occurs exclusively at Thr-881 in guard cells[75]. G26-51 exhibited inhibited phosphorylation of both Thr-881 and Thr-948 under blue light, and photosynthesis-induced Thr-881 phosphorylation (Fig. Ⅱ-2e-f and 4a). This observation suggests that the gene responsible for the G26-51 phenotype encodes a factor involved in Thr-881 and Thr-948 phosphorylation under both blue light and photosynthetic conditions. Although the kinase responsible for these phosphorylations remains unidentified, D-clade type 2C protein phosphatases (PP2C-D) are known to mediate their dephosphorylation[61,62,74]. Therefore, future studies should examine whether PP2C-D activity is constitutively altered in G26-51 and identify the responsible gene. Elevated CO_2

concentrations in leaves have been reported to induce Thr-948 dephosphorylation in guard cells, suggesting that reduced intercellular CO_2 concentration (Ci) due to mesophyll photosynthesis could promote Thr-948 phosphorylation[57]. Therefore, CO_2 response in G26-51 should be measured.

This study focused on the roles of Thr-881 and Thr-948 phosphorylation in blue light- and photosynthesis-dependent regulation. Other environmental cues may also influence H^+-ATPase activity through phosphorylation at additional sites beyond Thr-881 and Thr-948. For example, AHA2 Ser-931 is phosphorylated by PROTEIN KINASE SOS2-LIKES (PKS5), negatively regulating H^+-ATPase activation by weakening the interaction of the phosphorylated penultimate Thr with 14-3-3 protein[66]. Additionally, AHA2 Ser-899 phosphorylation in response to RAPID ALKALIZATION FACTOR (RALF) peptide results in H^+-ATPase inhibition[67]. These examples suggest that G26-51 has a mutation directly in the H^+-ATPase protein itself, and this possibility should be thoroughly investigated.

H^+-ATPase is regulated by various signals in diverse cell types[19]. Going forward, we will assess H^+-ATPase activation in various tissues and under different environmental signals in the G26-51 mutant.

Materials and Methods

Plant materials and growth conditions.

The *Arabidopsis thaliana* ecotype Columbia was used in all experiments and previously described mutants of *phot1-5 phot2-1*[44] were used. Ethyl methanesulfonate-mutagenized M2 seeds were purchased from Lehle Seeds or prepared by the Nisshoku Group.

Unless otherwise stated, plants were grown on soil:vermiculite (1:1) for 4 weeks under white light (50 μmol m^{-2} s^{-1}) with a 14/10 h light/dark cycle at 24°C. For thermal imaging, plants were grown on 0.8 % (w/v) agar plates containing half-strength Murashige–Skoog salts (pH 5.7), 2.3 mM MES, and 1 % (w/v) sucrose for 10 days under continuous white light. The plants were then transferred to a soil:vermiculite (1:1) mixture and further grown for 7 days under white light with a 13/11 h light/dark cycle.

Thermal imaging.

Leaf temperature was determined by infrared thermography (Infratec H2640-NEC / Avio). Plants were kept in the dark overnight at 20-24 °C with 50-60 % relative humidity and were then illuminated with RL (100 mmol m^{-2} s^{-1}) for 50 min. Then, a weak continuous BL (10 mmol m^{-2} s^{-1}) was superimposed on the RL[32]. Temperature decreases were visualized using thermal images, which were obtained by the subtraction of an image taken before the start of BL irradiation from one taken after 15-20 min of BL irradiation using InfReC Analyzer NS9500 Standard for image generation and Thermography Studio for image saving[32].

For trend analysis of whole leaf temperature, the temperatures of all pixels in the taken thermal images were converted to luminance values, histograms were generated, and threshold values were set using the Otsu method to distinguish between individual plants and the background. This process was performed for all images, and the temperature values of each pixel from the plant body area to the background area were averaged, and the background temperature value was subtracted from the plant body temperature value to extract and analyze the change in surface temperature every 30 sec in response to light.

Measurement of stomatal opening.

Stomatal conductance (g_s) of intact leaves was measured using a gas-exchange system (Li-6400; Li-Cor) under the following conditions: 350 ppm CO_2, 24 °C leaf temperature, 40–60% relative humidity, and 200 μmol m^{-1} flow rate. The leaves of dark-adapted plants were illuminated with red light (300 μmol m^{-2} s^{-1}) for 1 h, after which blue light (10 μmol m^{-2} s^{-1}) was superimposed on the background red light for 20 min.

For stomatal aperture measurements, the epidermis of dark-adapted plants was incubated in 5 mM MES-bistrispropane (pH 6.5), 50 mM KCl, and 0.1 mM $CaCl_2$ for 2 h in the dark or under red (50

μmol m^{-2} s^{-1}) and blue light (10 μmol m^{-2} s^{-1}). For Fc-incubated stomatal opening, the epidermis treated with 10 μM Fc in the buffer for 1 h in the dark. In case of intact leaves, they were incubated as well as the illumination of stomatal conductance and measured at each mentioned time. The stomatal aperture in the abaxial epidermis was observed using an inverted microscope (Eclipse TS100; Nikon) and quantified using the ImageJ 1.48 software (National Institutes of Health).

Isolation of guard cell protoplasts and measurement of H^+ pumping.

The guard cell protoplasts were enzymatically isolated from the fully developed leaves of 4-week-old *Arabidopsis* plants as described previously[35,47]. Blue light-dependent H^+ pumping from the guard cell protoplasts was measured using a glass pH electrode as described previously[47]. The guard cell protoplasts were incubated in 0.125 mM MES-NaOH (pH 6.0), 1 mM $CaCl_2$, 0.4 M mannitol, and 10 mM KCl under red light (300 μmol m^{-2} s^{-1}) for 2 h at 24 °C. Thereafter, a pulse of blue light (100 μmol m^{-2} s^{-1}, 30 s) was superimposed on the background red light.

Isolation of microsomal and soluble fractions from leaves.

Microsomal fractions were isolated from the leaves. The third or fourth leaves were homogenized with a mortar and pestle in an extraction buffer containing 50 mM MOPS-KOH (pH 7.5), 100 mM NaCl, 2.5 mM ethylenediamine-N,N,N',N'-tetraacetic acid (EDTA), 10 mM NaF, 5 mM dithiothreitol (DTT), 1 mM phenylmethylsulfonyl fluoride (PMSF), and 10 μM leupeptin. After centrifugation at 13,000 *g* for 10 min at 4 °C, the supernatants were further centrifuged at 100,000 *g* for 1 h at 4 °C, and the resulting pellet was resuspended in extraction buffer. This resuspended sample used as microsome fractions and supernatant sample used as soluble fractions.

Immunoblot analysis of guard cell proteins.

To determine the phosphorylation of plasma membrane H^+-ATPase, the guard cell protoplasts were incubated in 0.125 mM MES-NaOH (pH 6.0), 1 mM $CaCl_2$, 0.4 M mannitol, and 10 mM KCl under red light (300 μmol m^{-2} s^{-1}) for 30 min at 24 °C, after which a pulse of blue light (100 μmol m^{-2} s^{-1}, 30 s) was superimposed on the background red light. The reaction was terminated 3 min after the start of blue light illumination by adding trichloroacetic acid to the protoplast suspension. To measure the phosphorylation of phototropins or BLUS1, the reaction was ended 2 min. For Fc treatments, the guard cell protoplasts were preincubated under red light for 30 min, after which Fc was added to the final concentration of 10 μM. The protoplasts were further incubated in the dark for 3 min. For red light-induced phosphorylation of H^+-ATPase, the guard cell protoplasts were preincubated in the dark for 30 min and then illuminated under red light for 30 min.

Immunoblotting was performed as described previously[22,35] with slight modifications. Antibodies against phot1[77], phot2[78], BLUS1[32], the plasma membrane H^+-ATPase[75], and phospho-specific

antibodies against Thr-881[75] and Thr-948[75] of AHA1 and Ser-348[32] of BLUS1 have been described previously. Intensity of the protein bands was quantified using the ImageJ 1.48 software (National Institutes of Health).

Statistical analysis.

The data analyses carried out in this study were repeated and the obtained values are presented as means ± standard deviations (SD). Statistical analysis was performed using the analysis of variance (ANOVA) followed by Tukey's test in Excel 2007 (Microsoft) and Excel Toukei ver. 6.05 and Student's *t*-test in Excel 2021 (Microsoft). P value thresholds were $P < 0.05$ or $P < 0.01$.

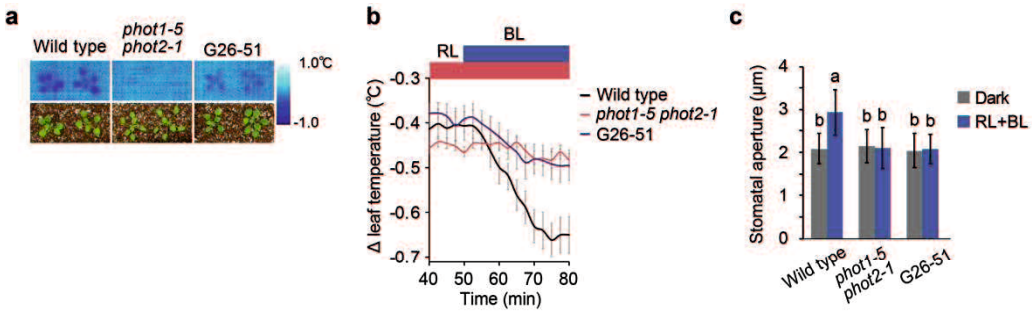

Fig. Ⅱ-1 Impairment of blue light-dependent stomatal opening.

a, b, Thermal image of a blue light-dependent leaf temperature decrease. Dark-adapted plants were illuminated with red light (RL: 100 μmol m^{-2} s^{-1}) for 50 min, and then blue light (BL: 10 μmol m^{-2} s^{-1}) was superimposed on RL. Subtractive images were obtained by subtracting an initial thermal image (before BL illumination) from an image taken 15 min after BL illumination (**a**). Trend analysis of whole leaf temperature changes every 30 seconds (**b**). **c,** Light-dependent stomatal opening in the epidermis. Epidermal strips were incubated in 5 mM MES-bistrispropane (pH 6.5), 50 mM KCl, and 0.1 mM CaCl2 in the dark or under RL (50 μmol m^{-2} s^{-1}) with or without BL (10 μmol m^{-2} s^{-1}) for 2 h. Data represent means ± SD (n = 75, pooled from triplicate experiments). Different letters indicate significant difference (ANOVA with Tukey's test, $P < 0.01$).

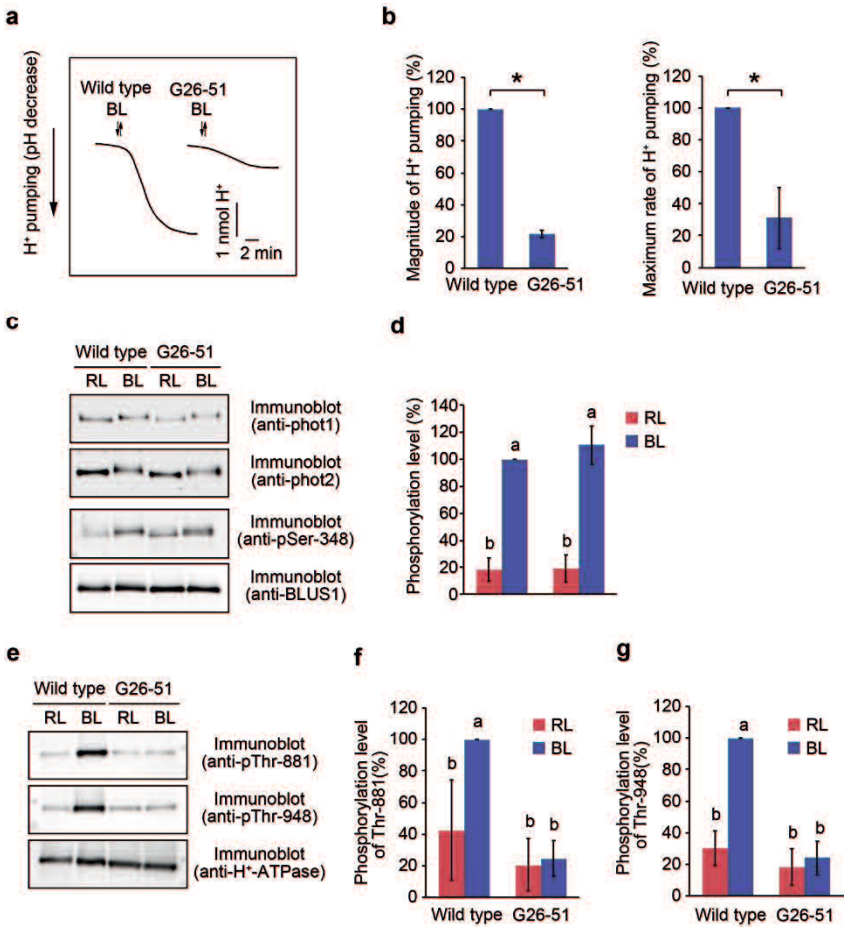

Fig. Ⅱ-2 Inhibition of H^+-ATPase activation in G26-51 mutant.

a, Blue light-induced H^+ pumping in guard cell protoplasts. Guard cell protoplasts were illuminated with RL (300 μmol m^{-2} s^{-1}) for 2 h, and then BL pulse (100 μmol m^{-2} s^{-1}, 30 s) was superimposed on RL as indicated. **b,** Quantification of the magnitude and maximum rate of H^+ pumping. Data represent means ± SD (n = 2 biologically independent experiments). Asterisk indicates significant difference from the wild-type (two-sided Student's t-test, $P < 0.05$). **c,** BL-dependent phosphorylation of phototropins (phot1, phot2) and BLUS1 in guard cells. The autophosphorylation of phototropins was determined by the upward electrophoretic mobility shift using anti-phot1 and anti-phot2 antibodies. The amount of BLUS1 and its phosphorylation ware detected using anti-BLUS1 and anti-Ser-348 antibodies. Each lane contained 5 mg of guard cell proteins. **e,** BL-dependent phosphorylation of H^+-ATPase. The amount of AHA1 and its phosphorylations ware detected using anti-AHA1, anti-Thr-881 and anti-Thr-948 antibodies. Each lane contained 4 mg of guard cell proteins. **d, f, g,** Quantification of the phosphorylation level of BLUS1 at Ser-348(**d**), AHA1 at Thr-881 (**f**) and Thr-948 (**g**). The data represent means ± SD (n = 3 biologically independent experiments). Different letters indicate significant differences (One-way ANOVA with Tukey's test, $P < 0.05$).

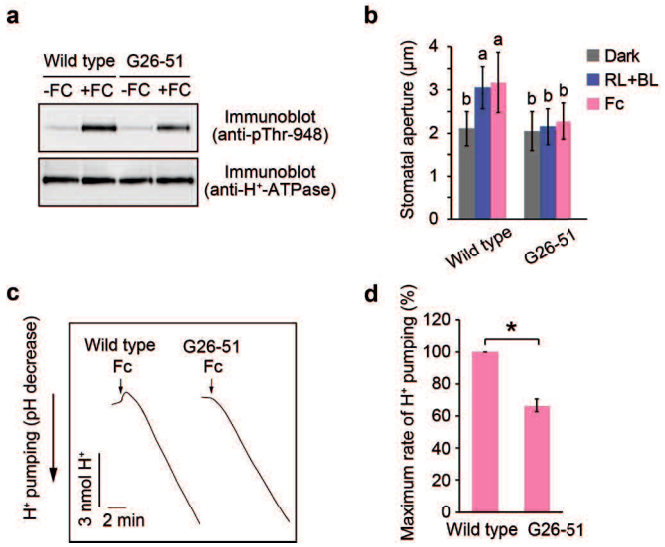

Fig. Ⅱ-3 Fc-induced H^+-ATPase activation and stomatal opening in G26-51 mutant.

a, Fc-dependent phosphorylation of H^+-ATPase. Fusicoccin (Fc) at 10 μM was added to the guard cell protoplasts and incubated in the dark for 3 min. Each lane contained 4 mg of guard cell proteins. **b,** Fc-dependent stomatal opening in the epidermis. Epidermal strips were incubated in 5 mM MES-bistrispropane (pH 6.5), 50 mM KCl and 0.1 mM CaCl2 in the dark or under RL (50 μmol m^{-2} s^{-1}) with or without BL (10 μmol m^{-2} s^{-1}) for 2 h. Fusicoccin (Fc) at 10 μM was added to the epidermis and incubated in the dark for 1 h. Data represent means ± SD (n = 75, pooled from triplicate experiments). Different letters indicate significant difference (ANOVA with Tukey's test, $P < 0.01$). **c,** Fc-dependent H^+ pumping in guard cell protoplasts. Guard cell protoplasts were illuminated by RL (300 mmol m^{-2} s^{-1}) for 2 h and added 10 μM Fc. **d,** Quantification of the maximum rate of H pumping by Fc. The data represent means ± SD ($n = 2$ biologically independent experiments). Asterisk indicates significant difference from the wild-type (two-sided Student's t-test, $P < 0.05$).

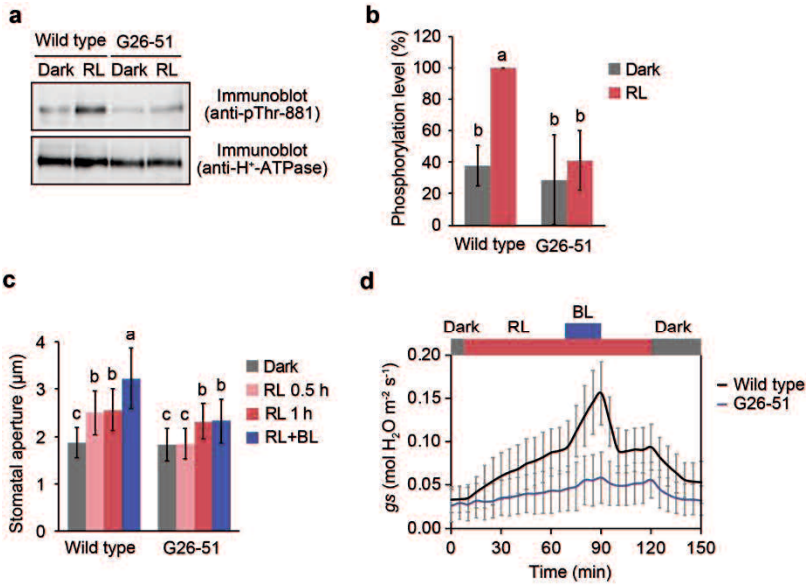

Fig. Ⅱ-4 G26-51 mutant showed suppression of red light response.

a, Red light-dependent phosphorylation of Thr-881. Guard cell protoplasts were incubated in the dark for 30 min or illuminated with red light (RL: 300 μmol m^{-2} s^{-1}) for 30 min. **b,** The relative phosphorylation levels of Thr-881 was quantified using the ImageJ software. The data represent means ± SD (n = 3 biologically independent experiments). Different letters indicate significant differences (One-way ANOVA with Tukey's test, $P < 0.05$). **c,** Light-dependent stomatal opening. Intact leaves were incubated in the dark or under RL (300 μmol m^{-2} s^{-1}) superimposition of BL (10 μmol m^{-2} s^{-1}). The data represent means ± SD (n = 75 stomata from three independent experiments). Different letters indicate significant differences (One-way ANOVA with Tukey's test, $P < 0.01$). **d,** Light-dependent changes in stomatal conductance in the intact leaves. Leaves of dark-adapted plants were illuminated with red light (RL: 300 μmol m^{-2} s^{-1}) for 1 h, after which blue light (BL: 10 μmol m^{-2} s^{-1}) was superimposed on RL for 20 min. The data represent means ± SD (n = 8 biologically independent plants).

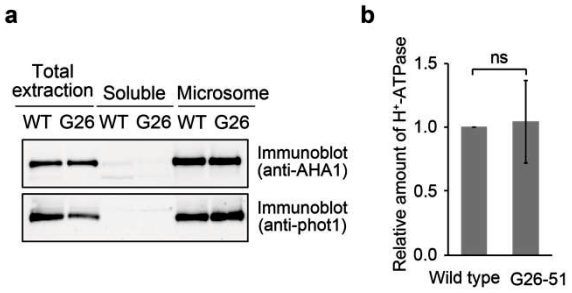

Fig. Ⅱ-5 The amount of AHA1 protein in microsome fractions in G26-51 mutant.

a, Immunoblot analysis using anti-H^+-ATPase antibodies. Each lane contains 15 μg of microsome sample or 45 μg of soluble and total extraction sample proteins. phot1 was used as the loading control. **b,** Quantification of the amount of H^+-ATPase in microsomal fractions using the ImageJ software. The amount of H^+-ATPase is expressed as a ratio of that in the wild-type. The data represent means ± SD (n = 2 biologically independent experiments). ns indicates no significant difference (two-sided Student's t-test, $P < 0.05$).

General discussion

In this study, Chapter I presents novel activation mechanisms of plasma membrane H^+-ATPase in response to blue light and guard cell photosynthesis, while Chapter II describes the isolation of a mutant involved in the activation of H^+-ATPase. However, the role of phosphorylated Thr-881 and Thr-948 in H^+-ATPase, specifically in conformational changes and activation, remains unknown. Structural analysis of yeast H^+-ATPase (PMA1) suggests that phosphorylation of Thr or Ser residues near Thr-881 in the R-1 region of the autoinhibitory domain induces a break in the salt bridges between the autoinhibitory and catalytic domains[50,51]. This could result in activation of H^+-ATPase through canceled chemical interference[50,51]. Furthermore, studies on *Nicotiana* H^+-ATPase have shown that phosphorylation of the Thr residue equivalent to Thr-948 leads to oligomerization through binding with the 14-3-3 protein, indicating that this phosphorylation event contributes to the stabilization of the active form of the enzyme[21,52].

Amino acids equivalent to Thr-881 and Thr-948 are conserved in almost all AHA isoforms, which are expressed throughout the plant[19]. These sites are also conserved from *Arabidopsis thaliana* to based land plants such as *Marchantia polymorpha* and some algae[16,19,79,80]. These findings suggest that Thr-881 and Thr-948 are important sites for H^+-ATPase activation. Further investigation is required to determine whether the activation mechanisms via phosphorylation of these Thr residues are conserved across these plants.

Thr-881 and Thr-948 in H^+-ATPase are reversible sites, with their phosphorylation states influenced by the surrounding environment. For example, phytohormone auxin has been reported to induce phosphorylation at these sites in stems and roots, while abiotic stress signals such as abscisic acid (ABA) and biotic stress signals like flg22 lead to dephosphorylation in Thr-948 and Thr-881, respectively[11,19]. These findings suggest that the phosphorylation states of Thr-881 and Thr-948 may reflect the activation level of H^+-ATPase, acting as a cross-talk point for various environmental signals.

We have isolated the G26-51 mutant, which regulate factors involved in blue and red light-induced phosphorylations of Thr-881 and Thr-948. However, the target gene in G26-51 remains unclear, and further investigation is needed to understand the underlying mechanisms regulating the phosphorylation of Thr-881 and Thr-948, including the role of protein kinases, phosphatases, and localization factors of AHAs. Moreover, it is essential to study whether the target gene controls the phosphorylation of AHA1 in response to other signals across various tissues and organs.

H^+-ATPase is an essential membrane protein that creates electrochemical potential by actively transporting H^+ across the membrane[12.] Thus, this study could contribute to the development of plants generating resource. In fact, plants that overexpress H^+-ATPase have been reported to exhibit facilitated stomatal opening and increased growth[81,82]. The T881D mutation, which substitutes aspartic acid for Thr-881, mimics the phosphorylated state and leads to enhanced H^+-ATPase activity and stomatal opening in the dark, without altering protein levels. This mutation also promotes stomatal

opening under light conditions compared to wild-type plants. These findings suggest that the T881D mutation could enhance CO_2 absorption and nutrients uptake. This study may be a stepping stone for applied research aimed at resolving energy and food security issues using the T881D mutation and the target gene in the G26-51 mutant.

References

1. Eberhard, S., Finazzi, G. & Wollman, F. The Dynamics of Photosynthesis. *Annu. Rev. Genet.* **42**, 463-515 (2008).
2. Hohmann-Marriott, M. F. & Blankenship, R. E. Evolution of Photosynthesis. *Annu. Rev. Plant Biol.* **62**, 515-548 (2011).
3. Hetherington, A. M. & Woodward, F. I. The role of stomata in sensing and driving environmental change. *Nature* **424**, 901-908 (2003).
4. Roelfsema, M. R. G. & Hedrich, R. In the light of stomatal opening: new insights into 'the Watergate'. *New Phytol.* **167**, 665-691 (2005).
5. Lawson, T. & Blatt, M. R. Stomatal size, speed, and responsiveness impact on photosynthesis and water use efficiency. *Plant Physiol.* **164**, 1556-1570 (2014).
6. Assmann, S. M. & Jegla, T. Guard cell sensory systems: recent insights on stomatal responses to light, abscisic acid, and CO_2. *Curr. Opin. Plant Biol.* **33**, 157-167 (2016).
7. Zhang, H. et al. Responses of woody plant functional traits to nitrogen addition: a meta-analysis of leaf economics, gas exchange, and hydraulic traits. *Front. Plant Sci.* **9**, 683 (2018).
8. Zhang, J., Chen, X., Song, Y. & Gong, Z. Integrative regulatory mechanisms of stomatal movements under changing climate. *J. Integr. Plant Biol*. **66**, 368–393 (2024).
9. Jezek, M. & Blatt, M. R. The membrane transport system of the guard cell and its integration for stomatal dynamics. *Plant Physiol.* **174**, 487-519 (2017).
10. Shimazaki, K., Doi, M., Assmann, S. M. & Kinoshita, T. Light regulation of stomatal movement. *Annu. Rev. Plant Biol.* **58**, 219-247 (2007).
11. Inoue, S. & Kinoshita, T. Blue light regulation of stomatal opening and the plasma membrane H^+-ATPase. *Plant Physiol.* **174**, 531-538 (2017).
12. Palmgren, M. G. Plant plasma membrane H^+-ATPases: powerhouses for nutrient uptake. *Annu. Rev. Plant. Physiol. Plant. Mol. Biol.* **52**, 817-845 (2001).
13. Robertson, W. R., Clark, K., Young, J. C. & Sussman, M. R. An *Arabidopsis thaliana* plasma membrane proton pump is essential for pollen development. *Genetics* **168**, 1677-1687 (2004).
14. Sondergaard, T. E., Schulz, A. & Palmgren, M. G. Energization of transport processes in plants. Roles of the plasma membrane H^+-ATPase. *Plant Physiol.* **136**, 2475-2482 (2004).
15. Grunwald, Y. et al. Arabidopsis leaf hydraulic conductance is regulated by xylem sap pH, controlled, in turn, by a P-type H^+-ATPase of vascular bundle sheath cells. *Plant J.* **106**, 301-313 (2021).
16. Pedersen, C. N., Axelsen, K. B., Harper, J. F. & Palmgren, M. G. Evolution of plant P-type ATPases. *Front. Plant Sci.* **3**, 31 (2012).
17. Pedersen, B. P., Buch-Pedersen, M. J., Morth, J. P., Palmgren, M. G. & Nissen, P. Crystal structure of the plasma membrane proton pump. *Nature* **450**, 1111-1114 (2007).

18. Palmgren, M. G., Sommarin, M., Serrano, R. & Larsson, C. Identification of an autoinhibitory domain in the C-terminal region of the plant plasma membrane H^+-ATPase. *J. Biol. Chem.* **266**, 20470-20475 (1991).
19. Falhof, J., Pedersen, J. T., Fuglsang, A. T. & Palmgren, M. Plasma membrane H^+-ATPase regulation in the center of plant physiology. *Mol. Plant* **9**, 323-337 (2016).
20. Nguyen, T. T., Blackburn, M. R. & Sussman, M. R. Intermolecular and intramolecular interactions of the *Arabidopsis* plasma membrane proton pump revealed using a mass spectrometry cleavable cross-linker. *Biochemistry* **59**, 2210-2225 (2020).
21. Ottmann, C. et al. Structure of a 14-3-3 coordinated hexamer of the plant plasma membrane H^+-ATPase by combining X-ray crystallography and electron cryomicroscopy. *Mol. Cell.* **25**, 427-440 (2007).
22. Kinoshita, T. & Shimazaki, K. Blue light activates the plasma membrane H^+-ATPase by phosphorylation of the C-terminus in stomatal guard cells. *EMBO J.* **18**, 5548-5558 (1999).
23. Svennelid, F. et al. Phosphorylation of Thr-948 at the C terminus of the plasma membrane H^+-ATPase creates a binding site for the regulatory 14-3-3 protein. *Plant Cell* **11**, 2379-2391 (1999).
24. Matthews, J. S. A., Vialet-Chabrand, S. & Lawson, T. Role of blue and red light in stomatal dynamic behaviour. *J. Exp. Bot.* **71**, 2253-2269 (2020).
25. Karlsson, P. E. Blue light regulation of stomata in wheat seedlings. I. Influence of red background illumination and initial conductance level. *Physiol. Plant.* **66**, 202-206 (1986).
26. Assmann, S. M. Enhancement of the stomatal response to blue light by red light, reduced intercellular concentrations of CO_2, and low vapor pressure differences. *Plant Physiol.* **87**, 226-231 (1988).
27. Lascève, G., Gautier, H., Jappé, J. & Vavasseur, A. Modulation of the blue light response of stomata of *Commelina communis* by CO_2. *Physiol. Plant.* **88**, 453-459 (1993).
28. Hosotani, S. et al. A BLUS1 kinase signal and a decrease in intercellular CO_2 concentration are necessary for stomatal opening in response to blue light. *Plant Cell* **33**, 1813-1827 (2021).
29. Briggs, W. R. & Christie, J. M. Phototropins 1 and 2: versatile plant blue-light receptors. *Trends Plant Sci.* **7**, 204-210 (2002).
30. Christie, J. M. Phototropin blue-light receptors. *Annu. Rev. Plant Biol.* **58**, 21-45 (2007).
31. Inoue, S. et al. Blue light-induced autophosphorylation of phototropin is a primary step for signaling. *Proc. Natl. Acad. Sci. U. S. A.* **105**, 5626-5631 (2008).
32. Takemiya, A. et al. Phosphorylation of BLUS1 kinase by phototropins is a primary step in stomatal opening. *Nat. Commun.* **4**, 2094 (2013).
33. Takemiya, A. et al. Reconstitution of an initial step of phototropin signaling in stomatal guard cells. *Plant Cell Physiol.* **57**, 152-159 (2016).
34. Takemiya, A., Kinoshita, T., Asanuma, M. & Shimazaki, K. Protein phosphatase 1 positively

regulates stomatal opening in response to blue light in *Vicia faba*. *Proc. Natl. Acad. Sci. U. S. A.* **103**, 13549-13554 (2006).

35. Takemiya, A., Yamauchi, S., Yano, T., Ariyoshi, C. & Shimazaki, K. Identification of a regulatory subunit of protein phosphatase 1 which mediates blue light signaling for stomatal opening. *Plant Cell Physiol.* **54**, 24-35 (2013).
36. Hayashi, M., Inoue, S., Ueno, Y. & Kinoshita, T. A Raf-like protein kinase BHP mediates blue light-dependent stomatal opening. *Sci. Rep.* **7**, 45586 (2017).
37. Hiyama, A. et al. Blue light and CO_2 signals converge to regulate light-induced stomatal opening. *Nat. Commun.* **8**, 1284 (2017).
38. Marten, H., Hedrich, R. & Roelfsema, M. R. G. Blue light inhibits guard cell plasma membrane anion channels in a phototropin-dependent manner. *Plant J.* **50**, 29-39 (2007).
39. Yang, Y. et al. The Ca^{2+} sensor SCaBP3/CBL7 modulates plasma membrane H^+-ATPase activity and promotes alkali tolerance in *Arabidopsis*. *Plant Cell* **31**, 1367-1384 (2019).
40. Wang, Z. F. et al. Receptor-like protein kinase BAK1 promotes K^+ uptake by regulating H^+-ATPase AHA2 under low potassium stress. *Plant Physiol.* **189**, 2227-2243 (2022).
41. Fuglsang, A. T. et al. Receptor kinase-mediated control of primary active proton pumping at the plasma membrane. *Plant J.* **80**, 951-964 (2014).
42. Yamauchi, S. et al. The plasma membrane H^+-ATPase AHA1 plays a major role in stomatal opening in response to blue light. *Plant Physiol.* **171**, 2731-2743 (2016).
43. Sugiyama, N. et al. Phosphopeptide enrichment by aliphatic hydroxy acid-modified metal oxide chromatography for nano-LC-MS/MS in proteomics applications. *Mol. Cell. Proteomics* **6**, 1103-1109 (2007).
44. Kinoshita, T. et al. Phot1 and phot2 mediate blue light regulation of stomatal opening. *Nature* **414**, 656-660 (2001).
45. Piette, A. S., Derua, R., Waelkens, E., Boutry, M. & Duby, G. A phosphorylation in the C-terminal autoinhibitory domain of the plant plasma membrane H^+-ATPase activates the enzyme with no requirement for regulatory 14-3-3 proteins. *J. Biol. Chem.* **286**, 18474-18482 (2011).
46. Rudashevskaya, E. L., Ye, J., Jensen, O. N., Fuglsang, A. T. & Palmgren, M. G. Phosphosite mapping of P-type plasma membrane H^+-ATPase in homologous and heterologous environments. *J. Biol. Chem.* **287**, 4904-4913 (2012).
47. Ueno, K., Kinoshita, T., Inoue, S., Emi, T. & Shimazaki, K. Biochemical characterization of plasma membrane H^+-ATPase activation in guard cell protoplasts of *Arabidopsis thaliana* in response to blue light. *Plant Cell Physiol.* **46**, 955-963 (2005).
48. Axelsen, K. B., Venema, K., Jahn, T., Baunsgaard, L. & Palmgren, M. G. Molecular dissection of the C-terminal regulatory domain of the plant plasma membrane H^+-ATPase AHA2: mapping of residues that when altered give rise to an activated enzyme. *Biochemistry* **38**, 7227-7234

(1999).

49. Nguyen, T. T., Sabat, G. & Sussman, M. R. In vivo cross-linking supports a head-to-tail mechanism for regulation of the plant plasma membrane P-type H^+-ATPase. *J. Biol. Chem.* **293**, 17095-17106 (2018).
50. Heit, S. et al. Structure of the hexameric fungal plasma membrane proton pump in its autoinhibited state. *Sci. Adv.* **7**, eabj5255 (2021).
51. Zhao, P. et al. Structure and activation mechanism of the hexameric plasma membrane H^+-ATPase. *Nat. Commun.* **12**, 6439 (2021).
52. Kanczewska, J. et al. Activation of the plant plasma membrane H^+-ATPase by phosphorylation and binding of 14-3-3 proteins converts a dimer into a hexamer. *Proc. Natl. Acad. Sci. U. S. A.* **102**, 11675-11680 (2005).
53. Serrano, E.E., Zeiger, E. & Hagiwara, S. Red light stimulates an electrogenic proton pump in *Vicia* guard cell protoplasts. *Proc. Natl. Acad. Sci. U. S. A.* **85**, 436-440 (1988).
54. Ando, E. & Kinoshita, T. Red light-induced phosphorylation of plasma membrane H^+-ATPase in stomatal guard cells. *Plant Physiol.* **178**, 838-849 (2018).
55. Fujita, T., Noguchi, K. & Terashima, I. Apoplastic mesophyll signals induce rapid stomatal responses to CO_2 in *Commelina communis*. *New Phytol*. **199**, 395-406 (2013).
56. Okumura, M., Inoue, S., Kuwata, K. & Kinoshita, T. Photosynthesis activates plasma membrane H^+-ATPase via sugar accumulation. *Plant Physiol.* **171**, 580-589 (2016).
57. Ando, E., Kollist, H., Fukatsu, K., Kinoshita, T. & Terashima, I. Elevated CO_2 induces rapid dephosphorylation of plasma membrane H^+-ATPase in guard cells. *New Phytol.* **236**, 2061-2074 (2022).
58. Suetsugu, N. et al. Guard cell chloroplasts are essential for blue light-dependent stomatal opening in Arabidopsis. *PLoS One* **9**, e108374 (2014).
59. Li, L. et al. Cell surface and intracellular auxin signalling for H^+ fluxes in root growth. *Nature* **599**, 273-277 (2021).
60. Lin, W. et al. TMK-based cell-surface auxin signalling activates cell-wall acidification. *Nature* **599**, 278-282 (2021).
61. Wong, J. H. et al. SAUR proteins and PP2C.D phosphatases regulate H^+-ATPases and K^+ channels to control stomatal movements. *Plant Physiol.* **185**, 256-273 (2021).
62. Akiyama, M. et al. Type 2C protein phosphatase clade D family members dephosphorylate guard cell plasma membrane H^+-ATPase. *Plant Physiol.* **188**, 2228-2240 (2022).
63. Pei, D. et al. Phosphorylation of the plasma membrane H^+-ATPase AHA2 by BAK1 is required for ABA-induced stomatal closure in Arabidopsis. *Plant Cell* **34**, 2708-2729 (2022).
64. Ogawa-Ohnishi M. et al. Peptide ligand-mediated trade-off between plant growth and stress response. *Science* **378**, 175-180 (2022).

65. Haruta, M., Gray, W. M. & Sussman, M. R. Regulation of the plasma membrane proton pump (H^+-ATPase) by phosphorylation. *Curr. Opin. Plant Biol.* **28**, 68-75 (2015).
66. Fuglsang, A. T. et al. *Arabidopsis* protein kinase PKS5 inhibits the plasma membrane H^+-ATPase by preventing interaction with 14-3-3 protein. *Plant Cell.* **19**, 1617-1634 (2007).
67. Haruta, M., Sabat, G., Stecker, K., Minkoff, B. B. & Sussman, M. R. A peptide hormone and its receptor protein kinase regulate plant cell expansion. *Science* **343**, 408-411 (2014).
68. Huala, E. et al. Arabidopsis NPH1: a protein kinase with a putative redox-sensing domain. *Science* **278**, 2120-2123 (1997).
69. Kagawa, T. et al. Arabidopsis NPL1: a phototropin homolog controlling the chloroplast high-light avoidance response. *Science* **291**, 2138-2141 (2001).
70. Kyono, Y., Sugiyama, N., Imami, K., Tomita, M. & Ishihama Y. Successive and selective release of phosphorylated peptides captured by hydroxy acid-modified metal oxide chromatography. *J. Proteome Res.* **7**, 4585-4593 (2008).
71. Nakagami, H. et al. Large-scale comparative phosphoproteomics identifies conserved phosphorylation sites in plants. *Plant Physiol*. **153**, 1161-1174 (2010).
72. Sakoda, K. et al. Higher stomatal density improves photosynthetic induction and biomass production in Arabidopsis under fluctuating light. *Front. Plant Sci.* **11**, 589603 (2020).
73. Okumura, M. & Kinoshita, T. Measurement of ATP hydrolytic activity of plasma membrane H^+-ATPase from *Arabidopsis thaliana* leaves. *Bio-protoc.* **6**, e2044 (2016).
74. Hayashi, Y. et al. Phosphorylation of plasma membrane H^+-ATPase Thr881 participates in light-induced stomatal opening. *Nat. Commun.* **15**, 1194 (2024).
75. Fuji, S. et al. Light-induced stomatal opening requires phosphorylation of the C-terminal autoinhibitory domain of plasma membrane H^+-ATPase. *Nat. Commun.* **15**, 1195 (2024).
76. Yamauchi, S. et al. Autophagy controls reactive oxygen species homeostasis in guard cells that is essential for stomatal opening. *Proc. Natl. Acad. Sci. U. S. A.* **116**, 19187-19192 (2019).
77. Doi, M., Shigenaga, A., Emi, T., Kinoshita, T. & Shimazaki, K. A transgene encoding a blue-light receptor, phot1, restores blue-light responses in the *Arabidopsis phot1 phot2* double mutant. *J. Exp. Bot.* **55**, 517–523 (2004).
78. Kong, S. G. et al. Blue light-induced association of phototropin 2 with the Golgi apparatus. *Plant J.* **45**, 994-1005 (2006).
79. Okumura, M. et al. Characterization of the Plasma Membrane H^+-ATPase in the Liverwort *Marchantia polymorpha*. *Plant Physiol.* **159,** 826-834 (2012).
80. Stéger, A. et al. The evolution of plant proton pump regulation via the R domain may have facilitated plant terrestrialization. *Commun. Biol.* **5,** 1312 (2022).

81. Zhang, M. et al. Plasma membrane H^+-ATPase overexpression increases rice yield via simultaneous enhancement of nutrient uptake and photosynthesis. *Nat Commun.* **12**, 735 (2021).
82. Wang, Y., Noguchi, K., Ono, N., Inoue, S., Terashima, I. & Kinoshita, T. Overexpression of plasma membrane H^+-ATPase in guard cells promotes light-induced stomatal opening and enhances plant growth. *Proc. Natl. Acad. Sci. U.S.A.* **111,** 533-538 (2014).

Acknowledgements

I would like to express my deepest gratitude to Prof. Atsushi Takemiya for guiding me in the study of light signal transduction in guard cells and allowing me to explore a world I could not have imagined when I first joined the plant cell signaling lab.

My heartfelt thanks go to the members of my thesis committee, Prof. Jun'ichi Mano, Prof. Kenji Matsui, Prof. Osami Misumi, and Prof. Ryosuke Mega, for their valuable insights and encouragement.

I am deeply grateful to Prof. Naoyuki Sugiyama and Dr. Asami Hiyama for their assistance with phosphoproteomic analysis, and to Dr. Yohei Kondo and Dr. Yoko Goto-Tomizawa for their support in constructing an automated analysis system for leaf surface temperature changes from thermal images. I would also like to thank Prof. Michito Tsuyama for experimental support and Prof. Takayuki Kohchi, Prof. Ryuichi Nishihama, and Prof. Ken-ichiro Shimazaki for their valuable advice. Additionally, I am thankful to Prof. Shota Yamauchi for his assistance and guidance with the experiments.

I am truly grateful to all the lab members, including Ms. Kyoka Tahara and Ms. Rio Matsumoto, who quietly supported me, as well as to my friends I met along the way, who have become invaluable companions in my pursuit of knowledge.

Finally, I would like to thank my family, who have always been there for me, for supporting my dreams wholeheartedly.